Lithospheric Research :

MT imaging of crust and mantle

Pascal Tarits
IUEM, Brest, France

Sophie Hautot (IMAGIR sarl), Noriko Tada (Jamstec, Japan)

Outline

- Some MT background
- 2-D/3-D modelling and inversion
- Joint inversion approach
- Regions where the approach will be tested (maybe)
  - Land MT: East African Rift
  - Marine MT: example of Society hotspot

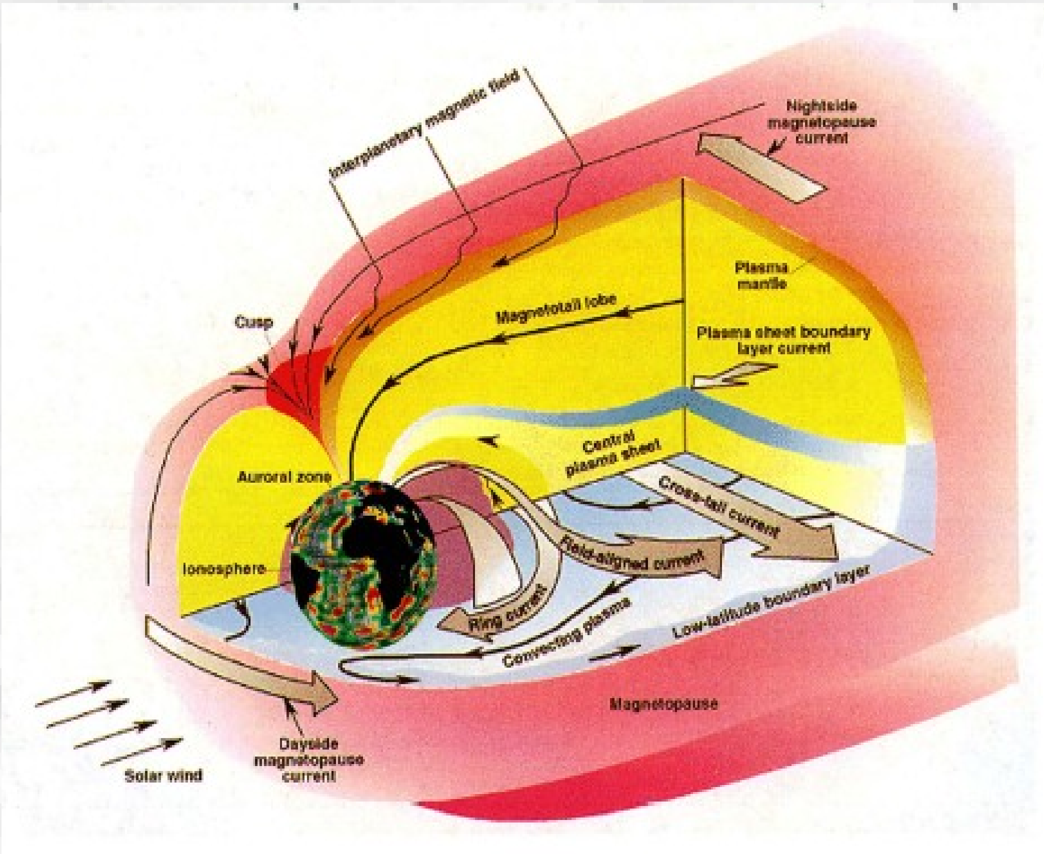

Source field in MT

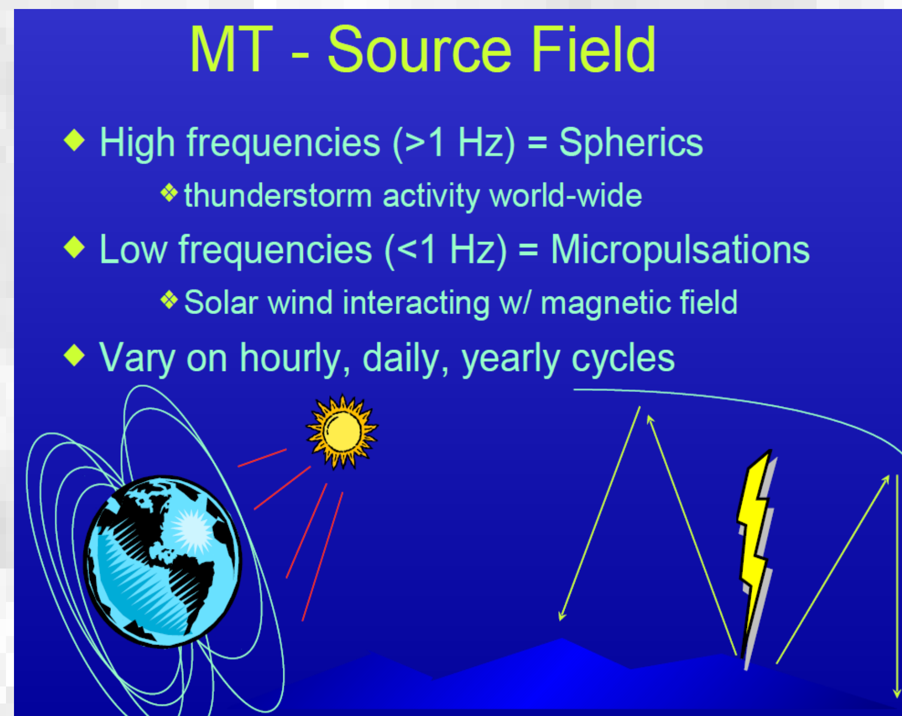

Electrical resistivity of rocks

(resistivity = 1 / conductivity)

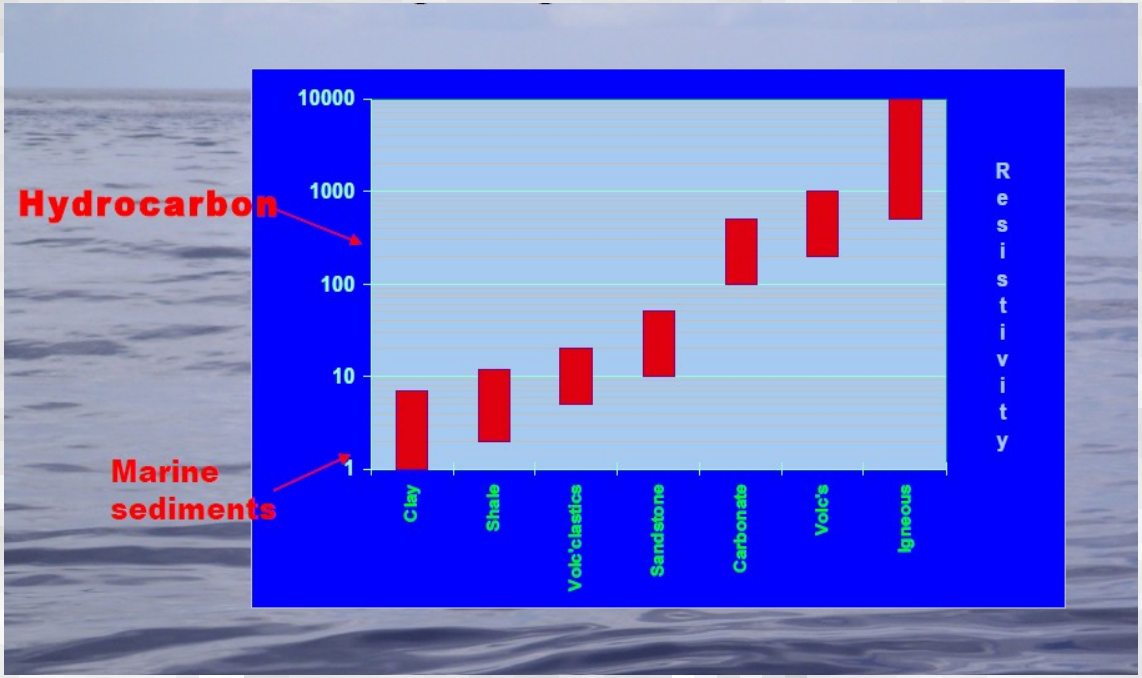

Rock type	Resistivity range (Ωm)
Granite porphyry	4.5×10^3 (wet) – 1.3×10^6 (dry)
Feldspar porphyry	4×10^3 (wet)
Syenite	$10^2 - 10^6$
Diorite porphyry	1.9×10^3 (wet) – 2.8×10^4 (dry)
Porphyrite	$10 - 5 \times 10^4$ (wet) – 3.3×10^3 (dry)
Carbonatized porphyry	2.5×10^3 (wet) – 6×10^4 (dry)
Quartz diorite	$2 \times 10^4 - 2 \times 10^6$ (wet) – 1.8×10^5 (dry)
Porphyry (various)	$60 - 10^4$
Dacite	2×10^4 (wet)
Andesite	4.5×10^4 (wet) – 1.7×10^2 (dry)
Diabase (various)	$20 - 5 \times 10^7$
Lavas	$10^2 - 5 \times 10^4$
Gabbro	$10^3 - 10^6$
Basalt	$10 - 1.3 \times 10^7$ (dry)
Olivine norite	$10^3 - 6 \times 10^4$ (wet)
Peridotite	3×10^3 (wet) – 6.5×10^3 (dry)
Hornfels	8×10^3 (wet) – 6×10^7 (dry)
Schists (calcareous and mica)	$20 - 10^4$
Tuffs	2×10^3 (wet) – 10^5 (dry)
Graphite schist	$10 - 10^2$
Slates (various)	$6 \times 10^2 - 4 \times 10^7$
Gneiss (various)	6.8×10^4 (wet) – 3×10^6 (dry)
Marble	$10^2 - 2.5 \times 10^8$ (dry)
Skarn	2.5×10^2 (wet) – 2.5×10^8 (dry)
Quartzites (various)	$10 - 2 \times 10^8$
Consolidated shales	$20 - 2 \times 10^3$
Argillites	$10 - 8 \times 10^2$
Conglomerates	$2 \times 10^3 - 10^4$
Sandstones	$1 - 6.4 \times 10^8$
Limestones	$50 - 10^7$
Dolomite	$3.5 \times 10^2 - 5 \times 10^3$
Unconsolidated wet clay	20
Marls	3 – 70
Clays	1 – 100
Oil sands	4 – 800

For reference:

Seawater : 0.25-0.33 Ω-m

Melt: 0.1-1 (silicate) to 0.005 Ω-m (carbonatite)

Atmosphere: ~10^{11} Ω-m

Maxwell's equations

$$\nabla \times \boldsymbol{E} = -\frac{\partial \boldsymbol{B}}{\partial t} - \frac{\partial \boldsymbol{M_b}}{\partial t}$$

$$\nabla \times \boldsymbol{H} - \frac{\partial \boldsymbol{D}}{\partial t} = \boldsymbol{J} + \boldsymbol{M_e}$$

$$\nabla \cdot \boldsymbol{B} = 0$$

$$\nabla \cdot \boldsymbol{D} = Q$$

Relationships with the physical parameters

$$\boldsymbol{J} = \sigma \boldsymbol{E}, \quad \boldsymbol{B} = \mu \boldsymbol{H}, \quad \boldsymbol{D} = \epsilon \boldsymbol{E}$$

Quantities σ, μ et ε (respectively electrical conductivity S/m or $\Omega^{-1}m^{-1}$, magnetic permeability H/m and electric permittivity F/m) are tensors in general

E electric field (V/m), ***B*** (T) magnetic induction, ***H*** (A/m) magnetic field, ***D*** deplacement current or dielectric field (C/m^2), ***J*** current density (A/m^2). The term Q is the density of elecric charges (q/m^2). The terms $\boldsymbol{M_e}$ and $\boldsymbol{M_b}$ represent current and fictive magnetic sources respectively.

Propagation or diffusion ?

$$\nabla \times \nabla \times \boldsymbol{E} + \mu_0 \epsilon_0 \frac{\partial^2 \boldsymbol{E}}{\partial t^2} + \mu_0 \sigma \frac{\partial \boldsymbol{E}}{\partial t} = \boldsymbol{0}$$

μ_0 et ε_0 are values in vacuum (4 π 10^{-7} SI and $1/(\mu_0 c^2)$, c speed of light).

Conductivity of earth materials are on average more than 10^{-5}-10^{-4} S/m, the characteristic frequencies measured in geophysical exploration are in general less than 10^5 Hz. Hence diffusion in MT is neglected

$$\frac{\partial^2 E_s}{\partial z^2} = \mu \sigma \frac{\partial E_s}{\partial t}$$

$$\frac{d^2 e_s}{d z^2} = i \omega \mu \sigma e_s$$

$$with\, e_s(z, \omega) = TF(E_s(z, t))$$

$$e_s(z>0, \omega) = e_s(z=0, \omega)\, \mathrm{e}^{-kz}$$

$$avec\ k = (i \omega \mu \sigma)^{1/2}\ et\ pdp = \sqrt{2/\omega \mu \sigma}$$

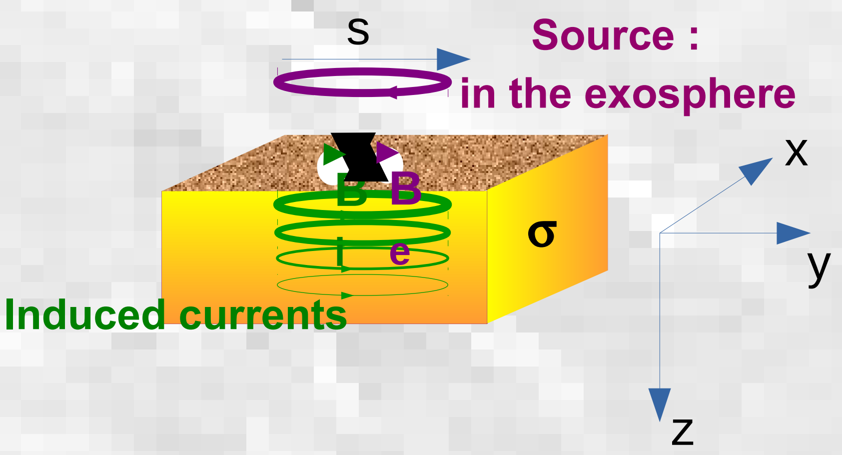

Pdp = penetration depth

Pdp = penetration depth

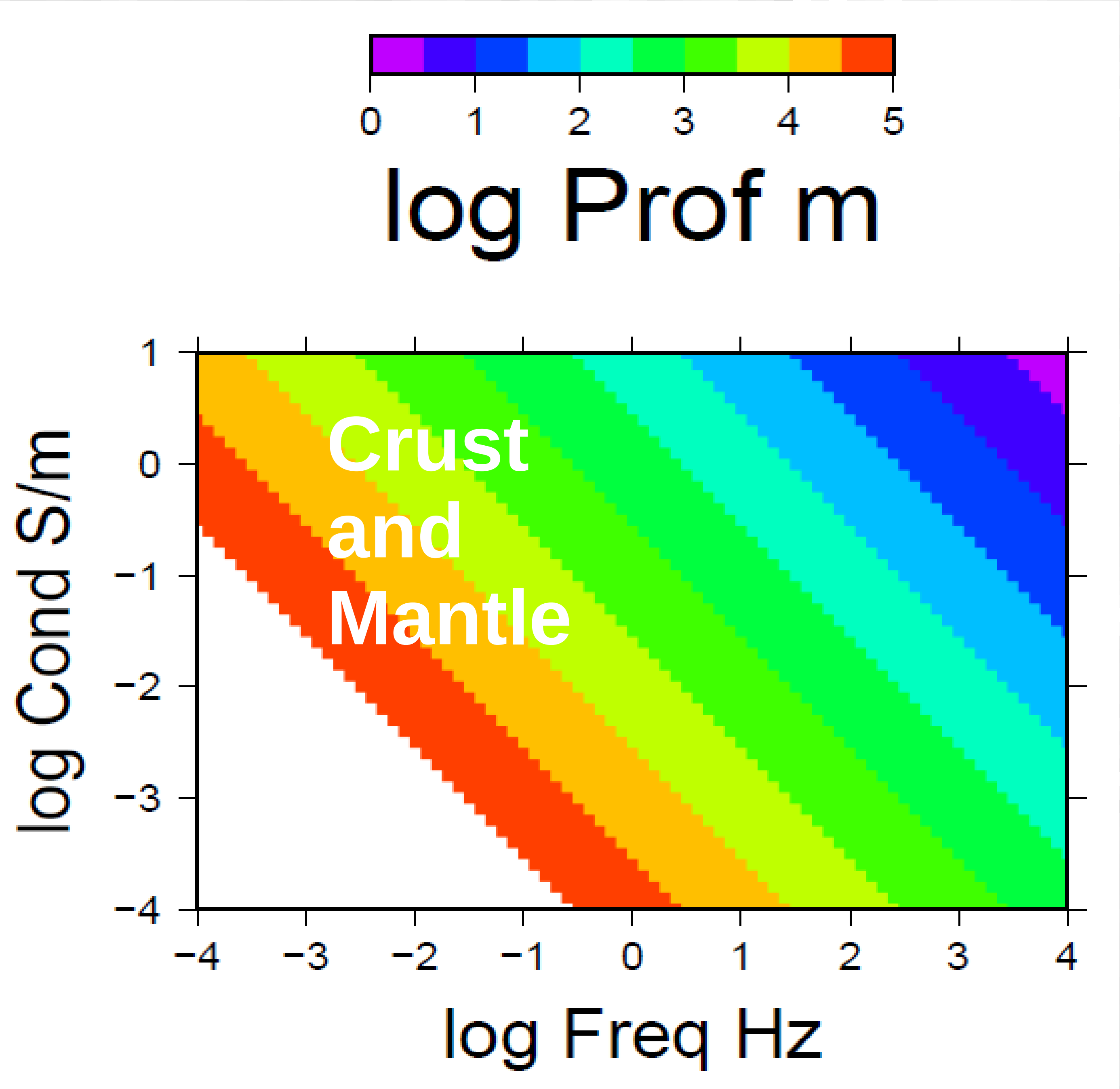

Definition of standard variables used in MT research

$$s=x \quad e_x=e_{x0}\mathrm{e}^{-kz}; by=-\frac{1}{i\omega}\frac{\partial e_x}{\partial z}=\frac{k}{i\omega}e_x$$

$$s=y \quad e_y=e_{y0}\mathrm{e}^{-kz}; bx=\frac{1}{i\omega}\frac{\partial e_y}{\partial z}=-\frac{k}{i\omega}e_y$$

$$Z_{xy}=\frac{e_x}{b_y}=\frac{i\omega}{k}=\sqrt{\frac{\omega}{\mu\sigma}}\,i^{1/2}$$

magnetotelluric impedance

$$Z_{yx}=\frac{e_y}{b_x}=-\frac{i\omega}{k}=\sqrt{\frac{\omega}{\mu\sigma}}\,(-i^{1/2})$$

$$\rho_a=\frac{\mu}{\omega}|Z_{xy}|^2=\frac{\mu}{\omega}|Z_{yx}|^2 \quad (\Omega\, m)$$

Apparent Resistivity

$$\Phi=arg(Z_{xy})$$

Phase

$\rho_a=1/\sigma$ and $\Phi=45°$ for an ½ space homogeneous and isotropic

Land MT Acquisition System

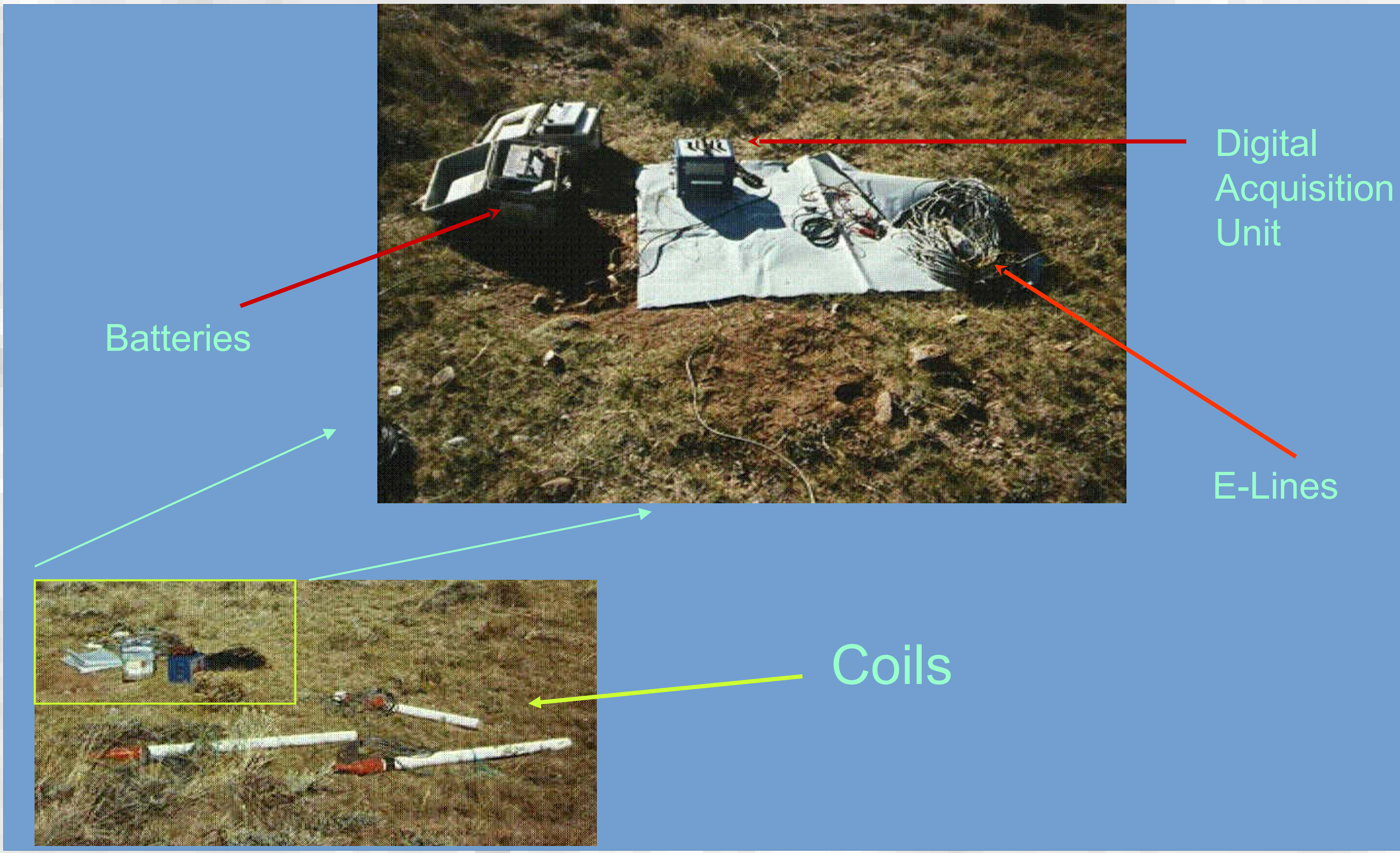

MT Layout

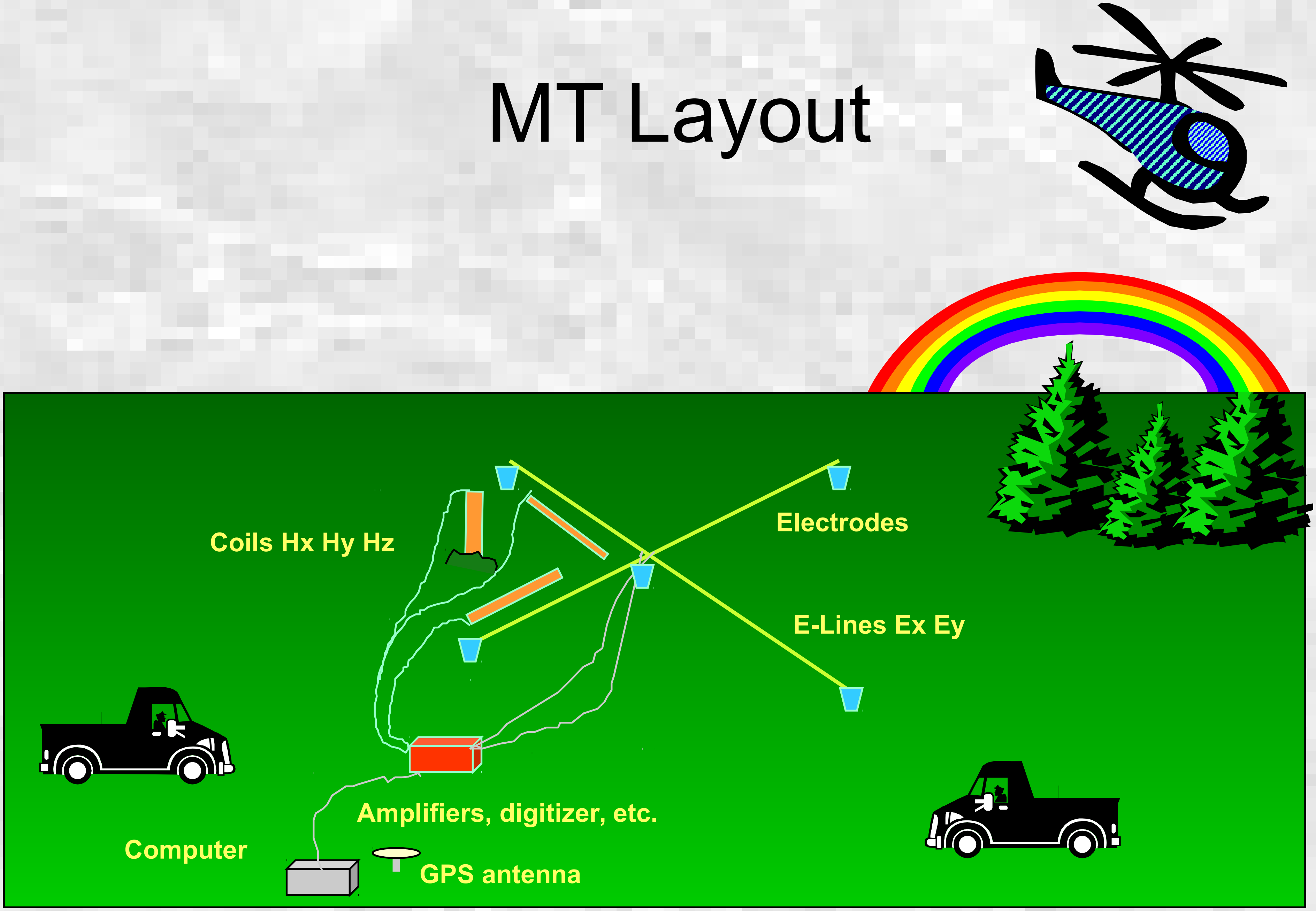

Courtesy K Christopherson, Chinook

MT Data record

This is an actual time series record, showing (from top) Ex, Ey, Hx, and Hy varying with time.

Note the correlation between Ex and Hy, and between Ey and Hx. Hz is not shown.

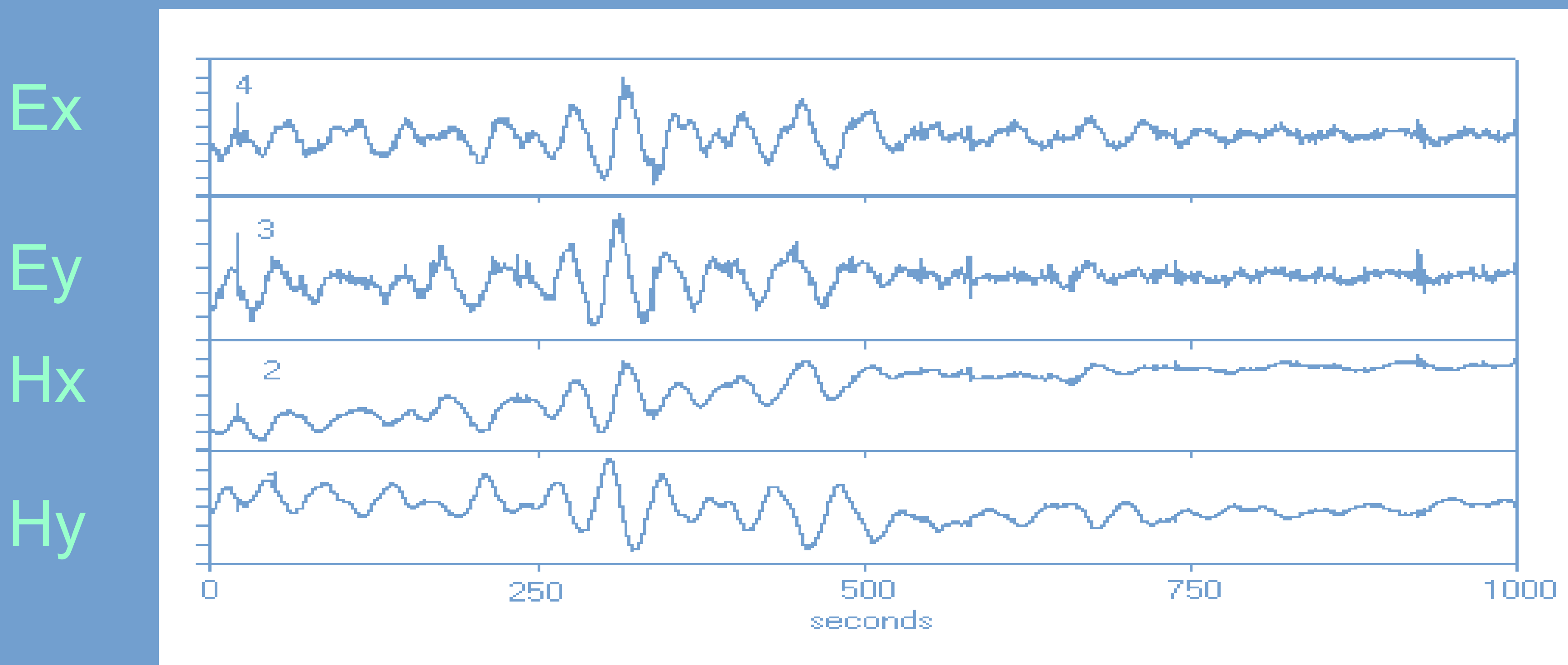

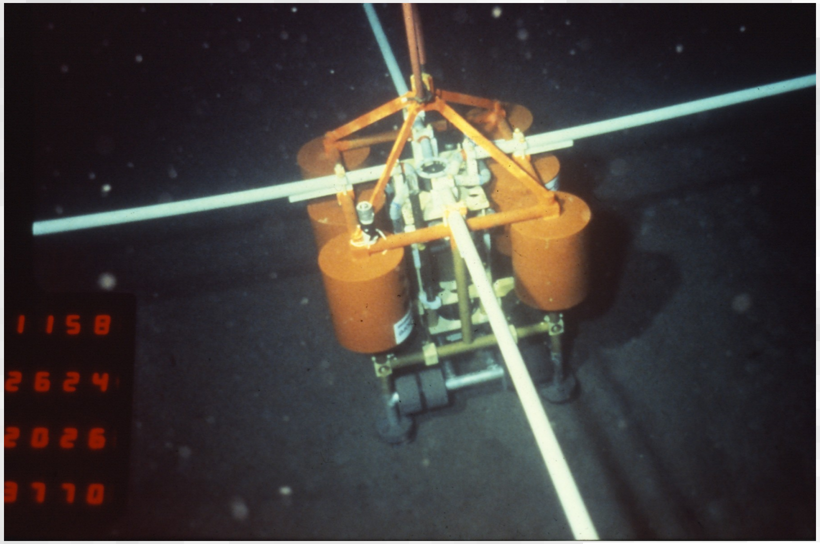

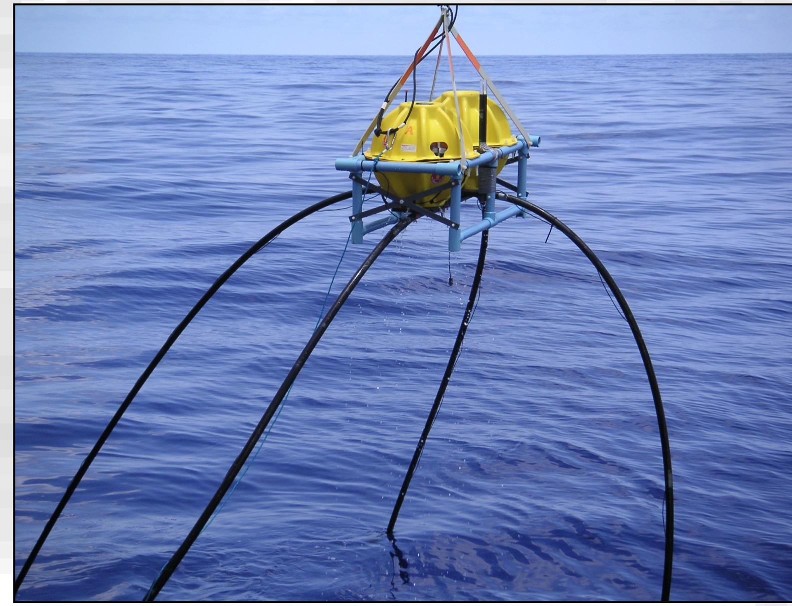

Marine MT for crust and mantle studies

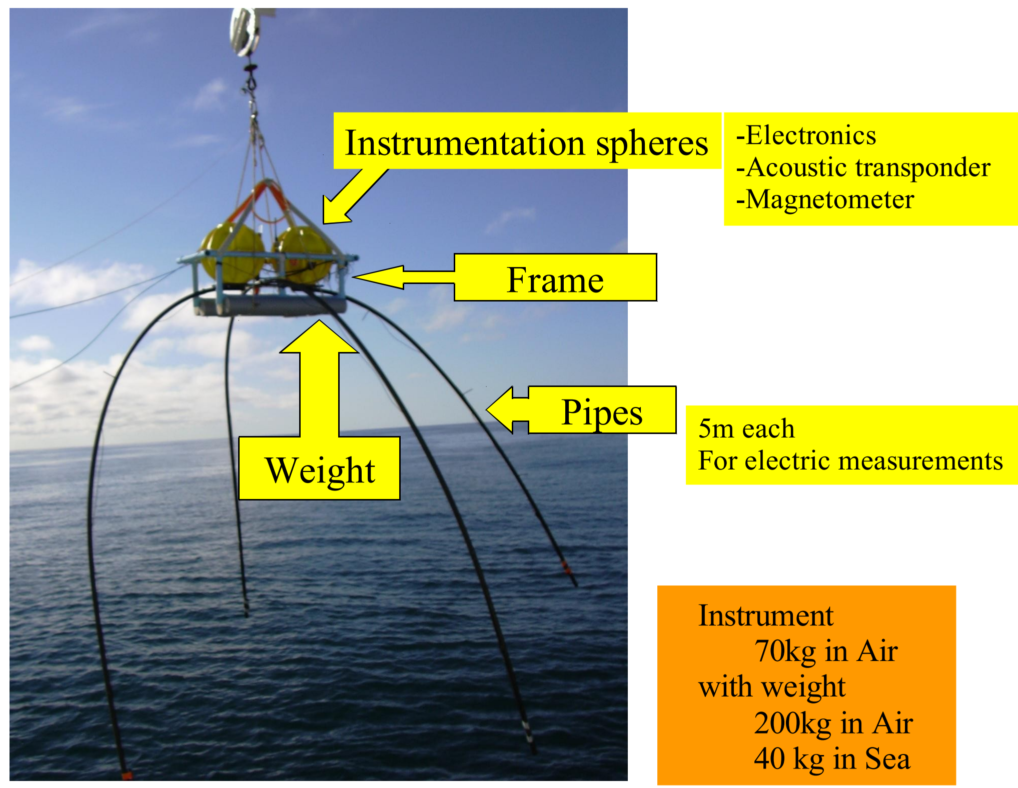

Specifics of Marine MT

- Water environment
- Water depth
- Bathymetry/coast
- Ocean currents

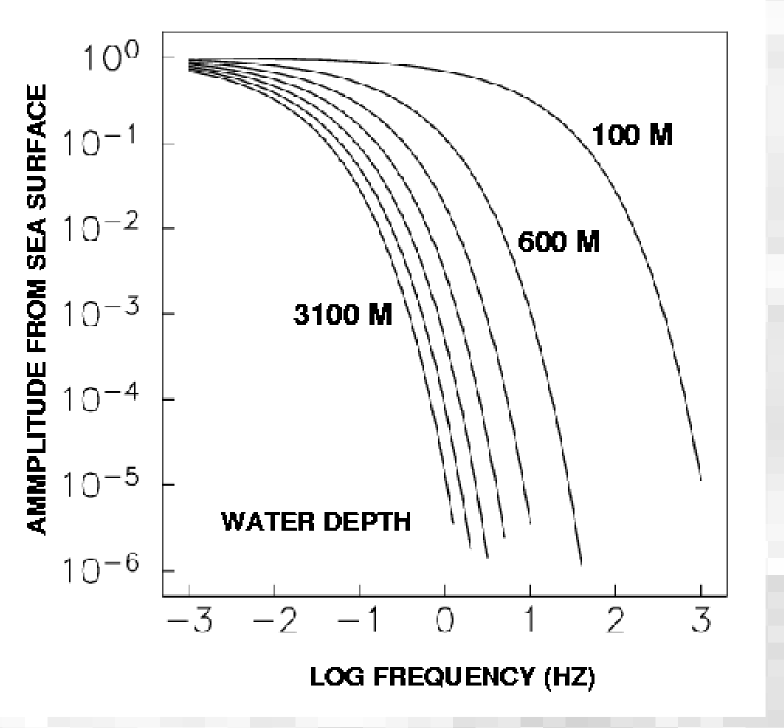

Sea-floor MT sounding

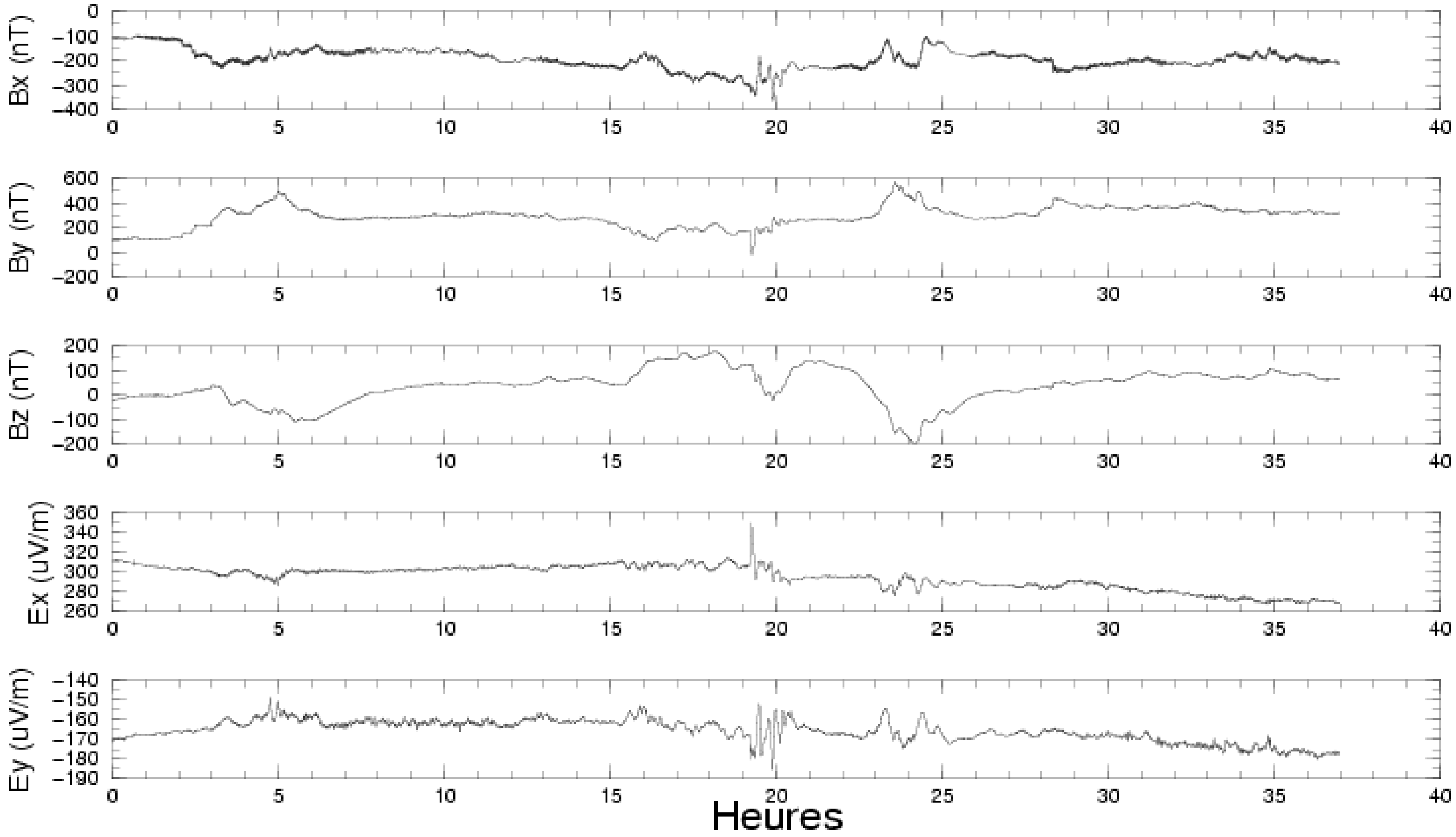

Water depth range
150-1400 m

Once you get your time series

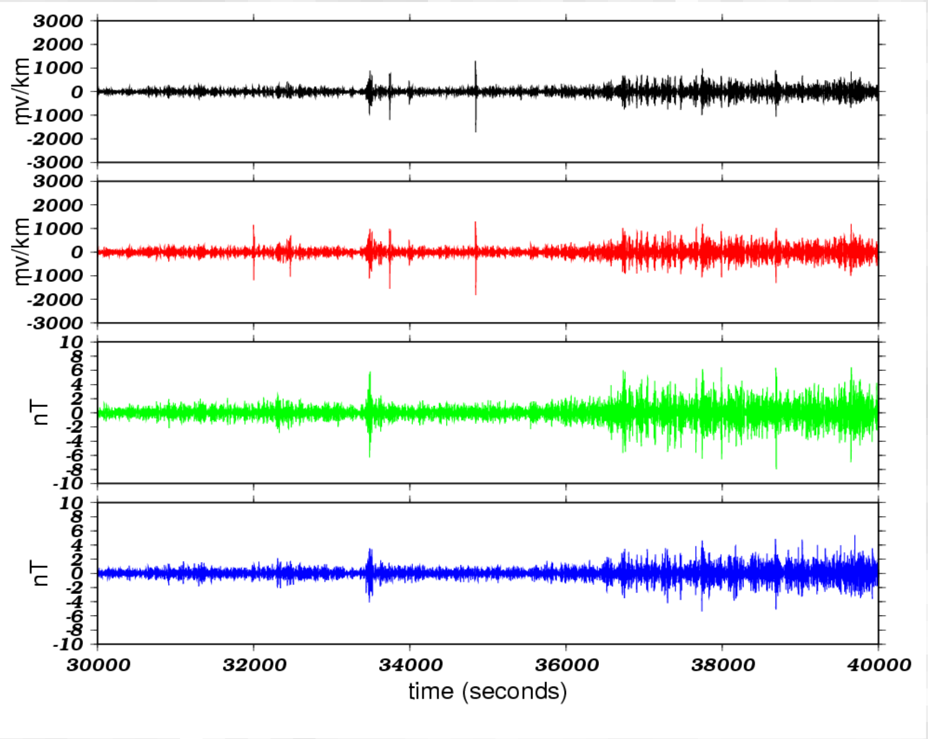

- **The time series are analysed in the frequency domain to derive the resistivity structure of the subsurface.**

$$\begin{pmatrix} E_x \\ E_y \end{pmatrix} = \begin{pmatrix} Z_{xx} & Z_{xy} \\ Z_{yx} & Z_{yy} \end{pmatrix} \begin{pmatrix} B_x \\ B_y \end{pmatrix}$$

- **The final data set to be inverted is the magnetotelluric tensor at as many frequencies as possible and at a number of sites (may be completed by tipper data)**

MT Data Curves

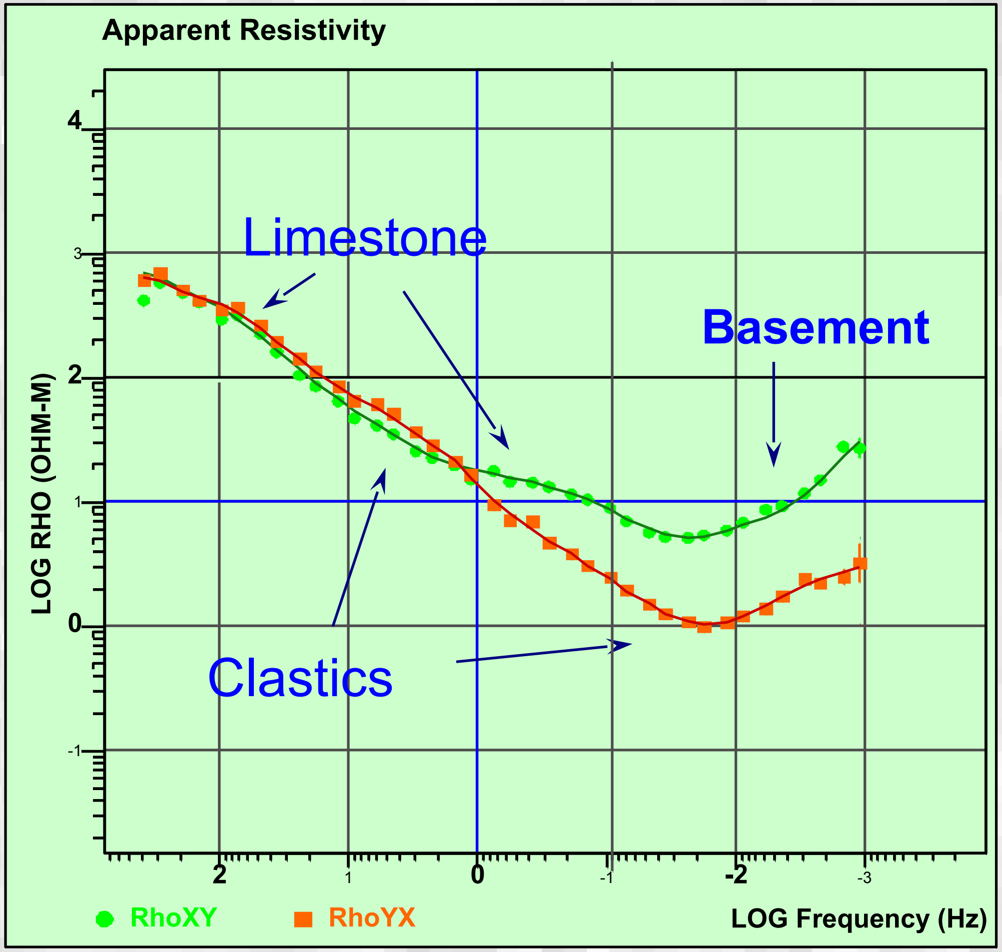

- Apparent resistivity
- Two curves, xy and yx
- Qualitative view of subsurface changes in resistivity
- Used with phase data for interpretation

Apparent resistivity varies with frequency because of change of resistivity with depth

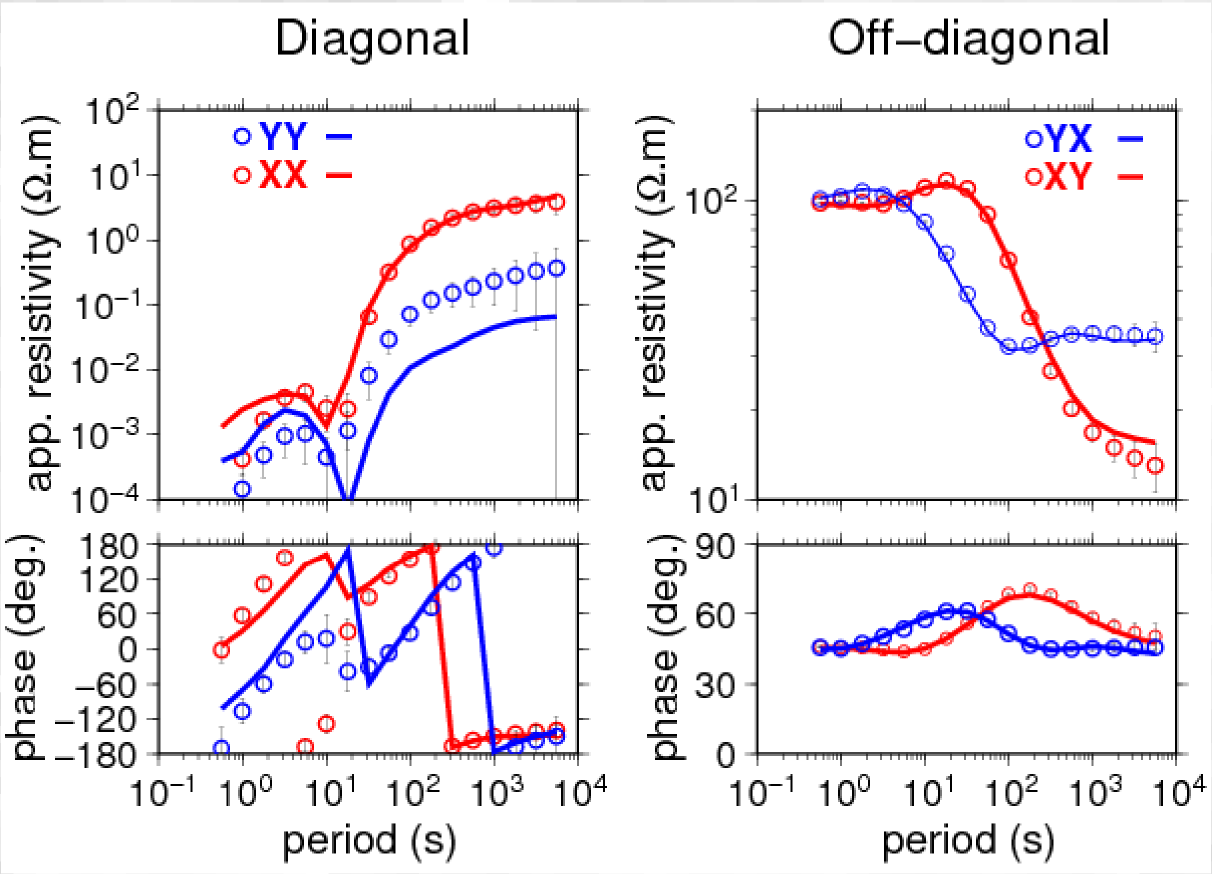

In general the 4 tensor components are non-zero because resistivity is 3-D

Magnetotelluric:
potentiel or imaging technique ?

Inversion of the magnetotelluric 1-D : a unique solution

The inverse problem for MT 1-D has an analytic solution. Starting from the impedance $Z(\omega) = F(\sigma(z))$, it is possible to derive uniquely $\sigma(z)=F^{-1}(Z(\omega))$ (Bailey 1970).

Above earth surface, $\sigma=0$ and **B** derives from a potentiel V which is the sum of the source potentiel Ve and the internal induced Vi

$$\nabla\times\boldsymbol{B}=\boldsymbol{0} \rightarrow \boldsymbol{B}=-\nabla V \quad et \quad V=V_e+V_i$$

Let λ be a wave number and define K_λ=Vi/Ve (which par continuity of Ve and Vi at z=0 may be expressed as a function of the impedance MT Z. Bailey established the following equations:

$$\frac{dK_\lambda}{dz}=-4\pi\lambda K_\lambda-\frac{i\omega\sigma(z)}{\lambda}(K_\lambda-1)^2$$

For σ bounded, real, analytic and no zero.

$$\sigma(z)=4\pi^2\lambda^2\left[2\int_0^\infty \Re(K_\lambda-1)^2 d\omega\right]^{-1}$$

In practice, this equation is difficult to use (Achache et al 1981 did it for 1-D global) because data has a limited bandwith and noise (endemic in inversion). Partial mathematical proofs in 2-D and 3-D have been studied for ideal cases

MT inversion is non-linear

$$\nabla \times \boldsymbol{E}(\boldsymbol{r}, \sigma) = -\frac{\partial \boldsymbol{B}}{\partial t}(\boldsymbol{r}, \sigma)$$

$$\nabla \times \boldsymbol{B}(\boldsymbol{r}, \sigma) = \mu \sigma(\boldsymbol{r}) \boldsymbol{E}(\boldsymbol{r}, \sigma)$$

Classical and statistical approaches

Bayesian, genetic, quasi analytic solutions have been developpend in 1-D, rarely in 2-D. All but a few practical MT inverse solutions are classical in 3-D. A cost function U is minimized, usually a weighted χ2 by a regularisation term R times a Lagrange parameter λ:

$$U = \|\boldsymbol{W}(\boldsymbol{d} - \boldsymbol{F}(\boldsymbol{m}))\|^2 + \lambda R(\boldsymbol{m})^2$$

W is the data covariance **d** et **m** the model parameters. **F** is the response du model. Regularisation is the key and a very large number of approaches have been proposed.

The earth in 2-D

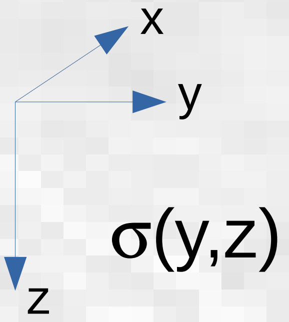

For a plane wave, the 2-D approximation decouples the Maxwell equations:

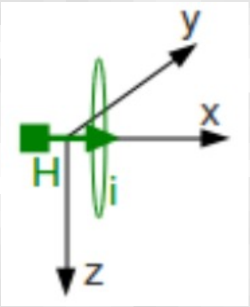

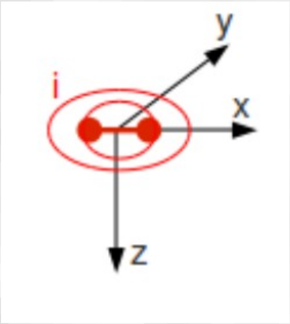

$$MODE\ H-POL(TM)$$
$$\partial_y e_z - \partial_z e_y = -i\omega b_x$$
$$\partial_z b_x = \mu\sigma e_y$$
$$-\partial_y b_x = \mu\sigma e_z$$

$$MODE\ E-POL(TE)$$
$$\partial_z e_x = -i\omega b_y$$
$$-\partial_y e_x = -i\omega b_z$$
$$\partial_y b_z - \partial_z b_y = \mu\sigma e_x$$

subsitute ez and ey

$$\partial_y \frac{\partial_y b_x}{\mu\sigma} + \partial_z \frac{\partial_z b_x}{\mu\sigma} = i\omega b_x$$

subsitute bz and by

$$\partial_y^2 e_x + \partial_z^2 e_x = i\omega\mu\sigma e_x$$

The decoupling disappears if conductivity is anisotropic and/or medium is 3-D

Criteria to design a grid (for forward or inverse)

Criteria are in general base on minimum maximum pdps

The physics is the physics of diffusion

Meshes size vary with depth and (for inverse) number of observation sites.

Lateral boundaries must be far away (diffuse away until vanish)

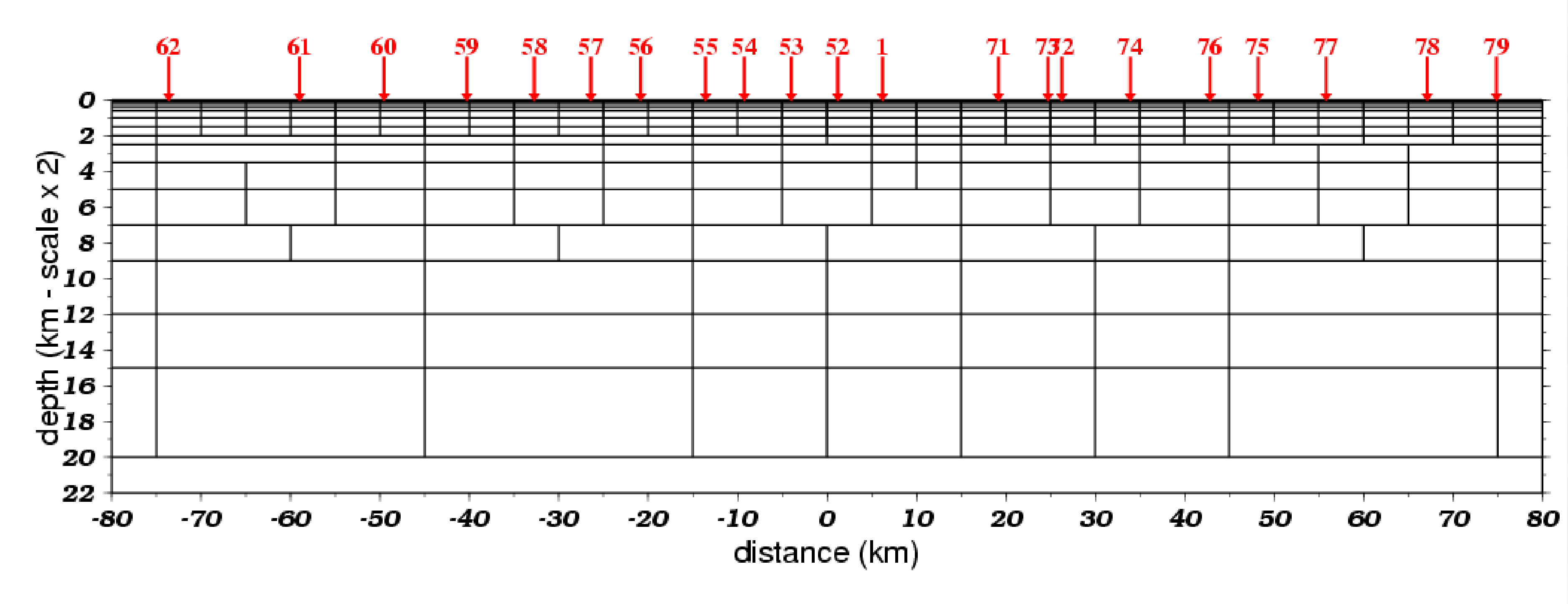

Limitation of 2-D analysis

The existence of lateral variation of conductivity in our earth model introduces a new term in the solutions.

Electric charges accumulate at lateral conductivity contrasts and generates an emf that at minima offsets the observed field (static shift) and in general may induces eddy currents.

$$\nabla\cdot\boldsymbol{J}=0 \rightarrow \nabla\sigma(\boldsymbol{r})\cdot\boldsymbol{E}=0 \rightarrow \sigma\nabla\cdot\boldsymbol{E}+\nabla\sigma\cdot\boldsymbol{E}=0$$

$$\rightarrow \nabla\cdot\boldsymbol{E}=Q/\epsilon=-\frac{\nabla\sigma}{\sigma}\cdot\boldsymbol{E}$$

$$\boldsymbol{E}=-\frac{1}{4\pi\epsilon}\nabla\int Q/R\,dV$$

This effect may be quite strong locally and bias the 2-D MT field by 3-D distorsion

An example of intense static distorsion

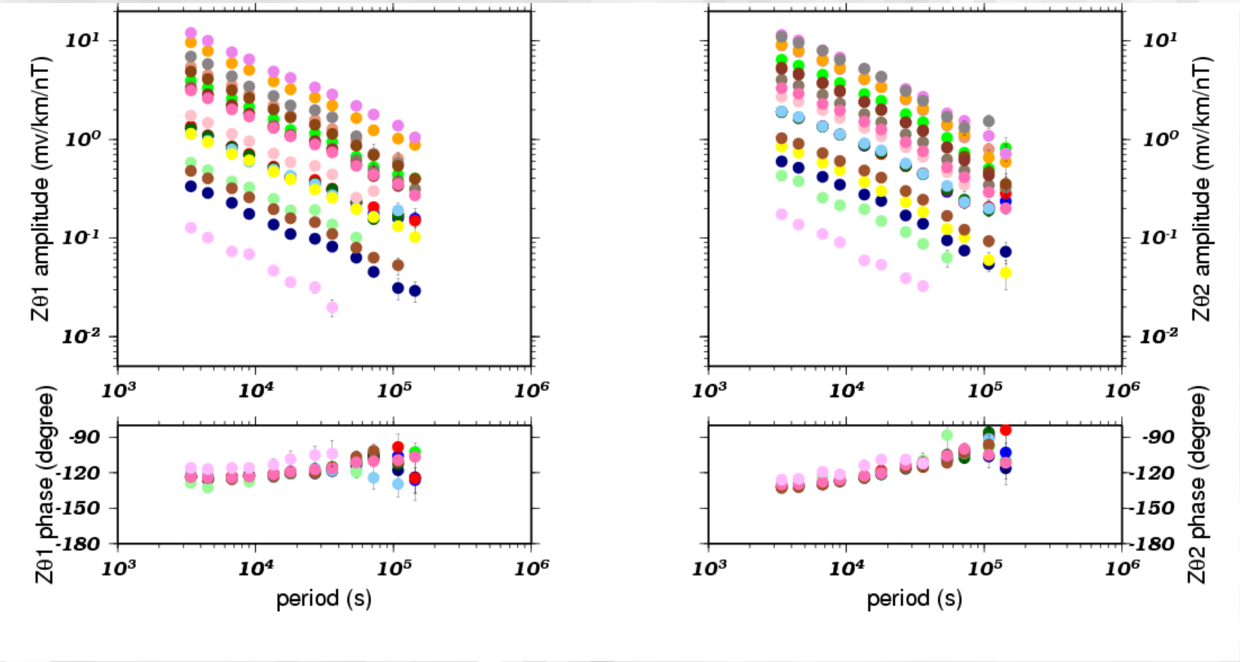

At a same site, the observed impedance changes dramatically according to the direction along which the electric field is observed suivant différentes direction du champ électrique

The 2-D approach is now becoming out of date with the emergence of 3-D inversion getting more and more popular because the distortion is included in the inversion

- A few 3D inversion codes exist, mainly for industry but also for academic *(e.g., Newman and Alumbaugh (2000), Mackie et al. (2001), Sasaki (2004), Siripunvaraporn et al. (2005), Hautot and Tarits (2009), Avdeev and Avdeeva (2009), Zhdanov et al. (2011), Egbert and Kelbert (2012), and others...).*

Only two are accessible to research:

http://blogs.oregonstate.edu/modem3dmt/

http://mucc.mahidol.ac.th/~scwsp/wsinv3dmt/

In Crust and Mantle MT studies, data are scarce, unevenly distributed or along a profile

- **The inversion technique is based on minimization of an error function between the observed data and the model response using a downhill descent technique**

Advantages of the downhill descent technique:

- Grid defined in data-space matrices

- No need for strong smoothness constraints

- Only forward calculation is needed, no gradient or hessian

- For joint inversion, forward and inverse grid are independent so any solvers may be mixed

Drawback

The difficulty is that for a large data set:

- The number of parameters is large

- Many calls to the forward solver

The 3D MT inversion method with MINIM3D

- The 3D inversion technique is based on an iterative procedure
- Each iteration is a call to a forward solver
(here 3D FD code (Mackie et al., 1993))
- Minimization of an error function between the observed data and the model response using a downhill descent technique
- The data are the 4 complex elements of the MT tensor at all available frequencies (plus tipper if available)

Application to real data sets: non regular MT site array

In order to reduce the number of parameters (the number of calls), the grid used for the inversion is different from the grid used for the forward calculation

The parameters are adjusted to the sensitivity of the MT data:

- Uppermost layers:
The data constrain short distance structures only
The size of the blocks increase with the distance from the MT sites

- Deeper layers:
The resolution decrease with depth
The size of the blocks is larger

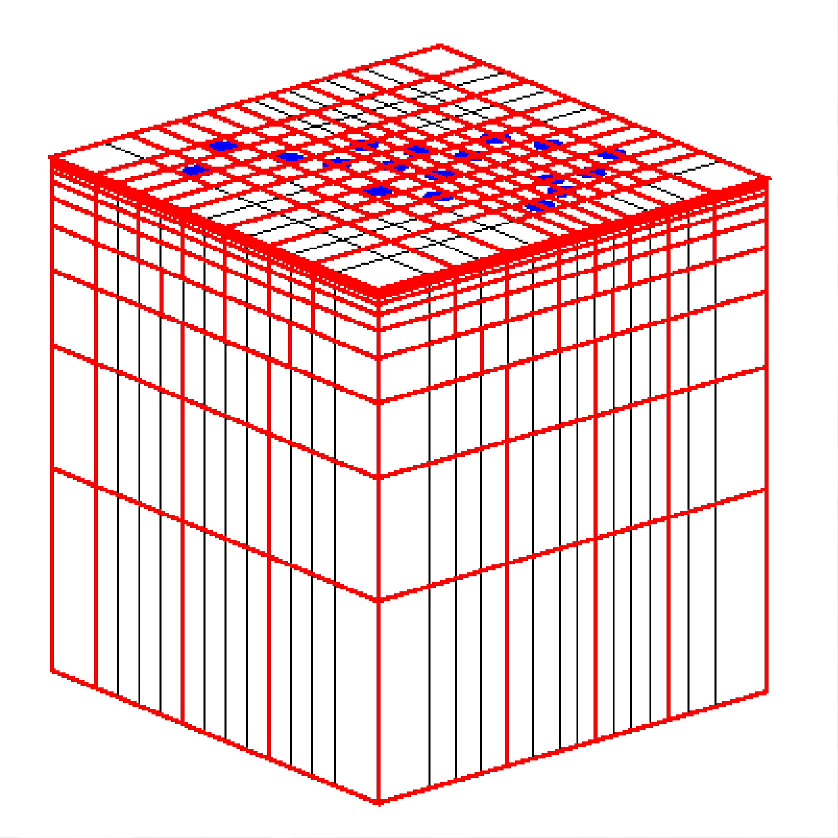

Non-regular array of MT sites: Case Study 1
The Omo Basin, South-West Ethiopia

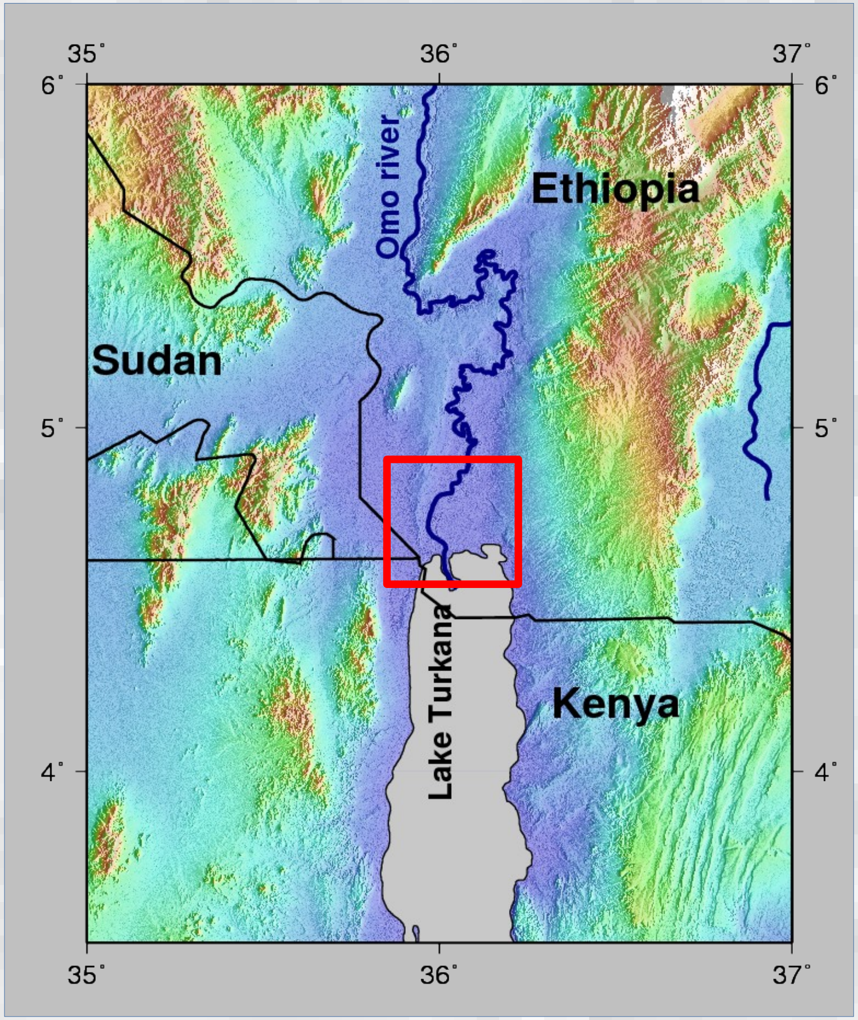

Aim of the study: Understanding of the regional geometry of a rift basin for the purpose of petroleum exploration

Non-regular array of MT sites: Case Study 1
The Omo Basin, South-West Ethiopia

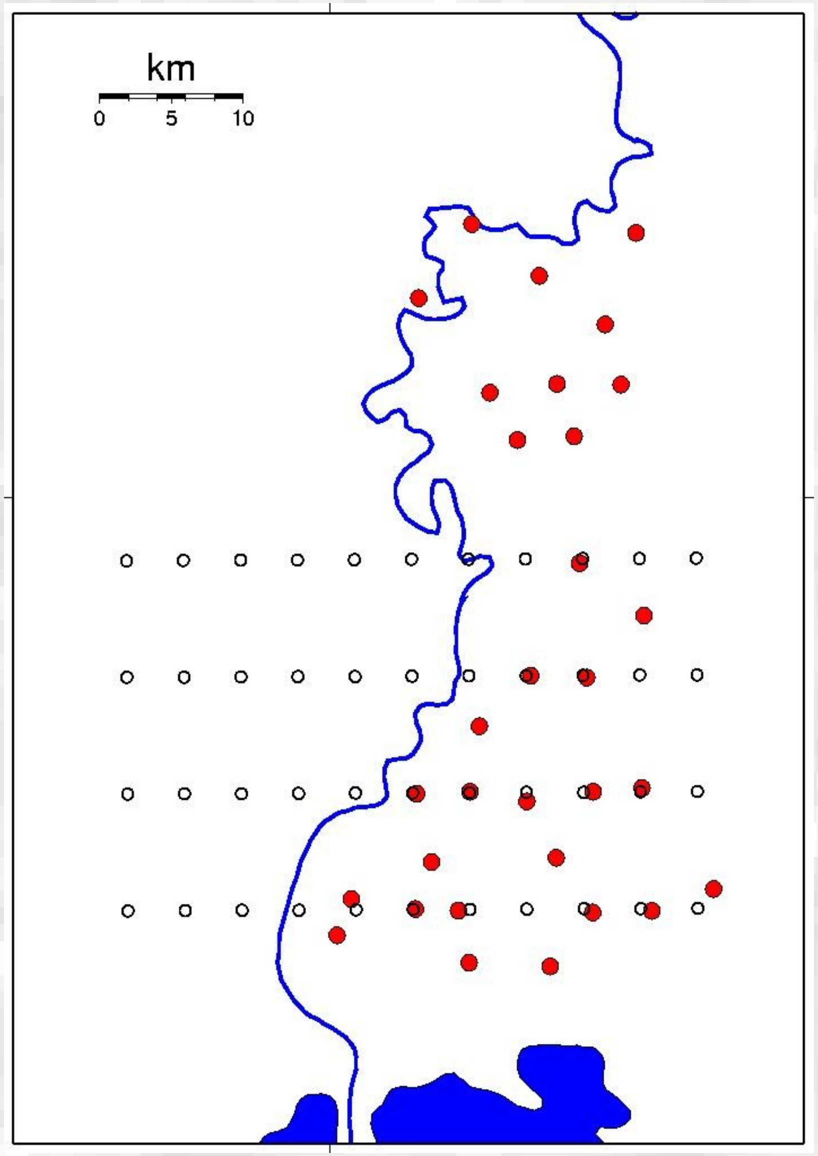

Non-regular array of MT sites: Case Study 1
The Omo Basin, South-West Ethiopia

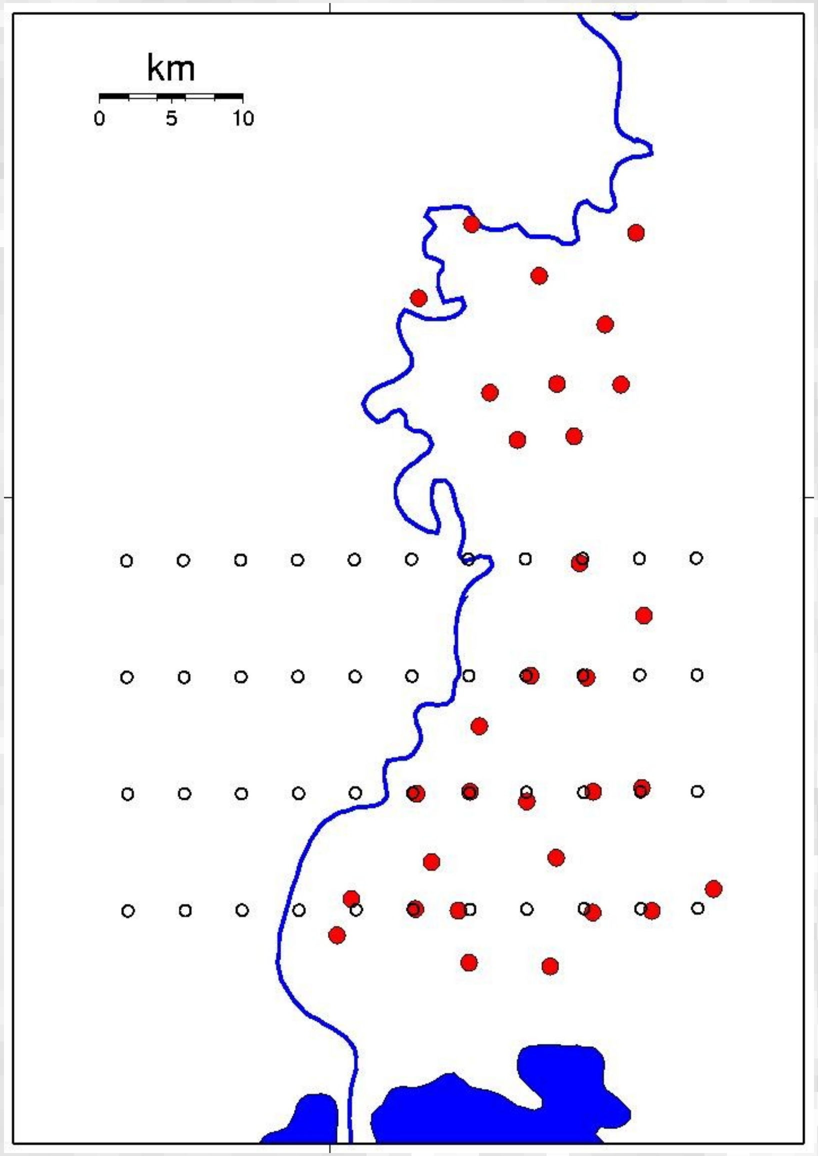

Grid for forward computation

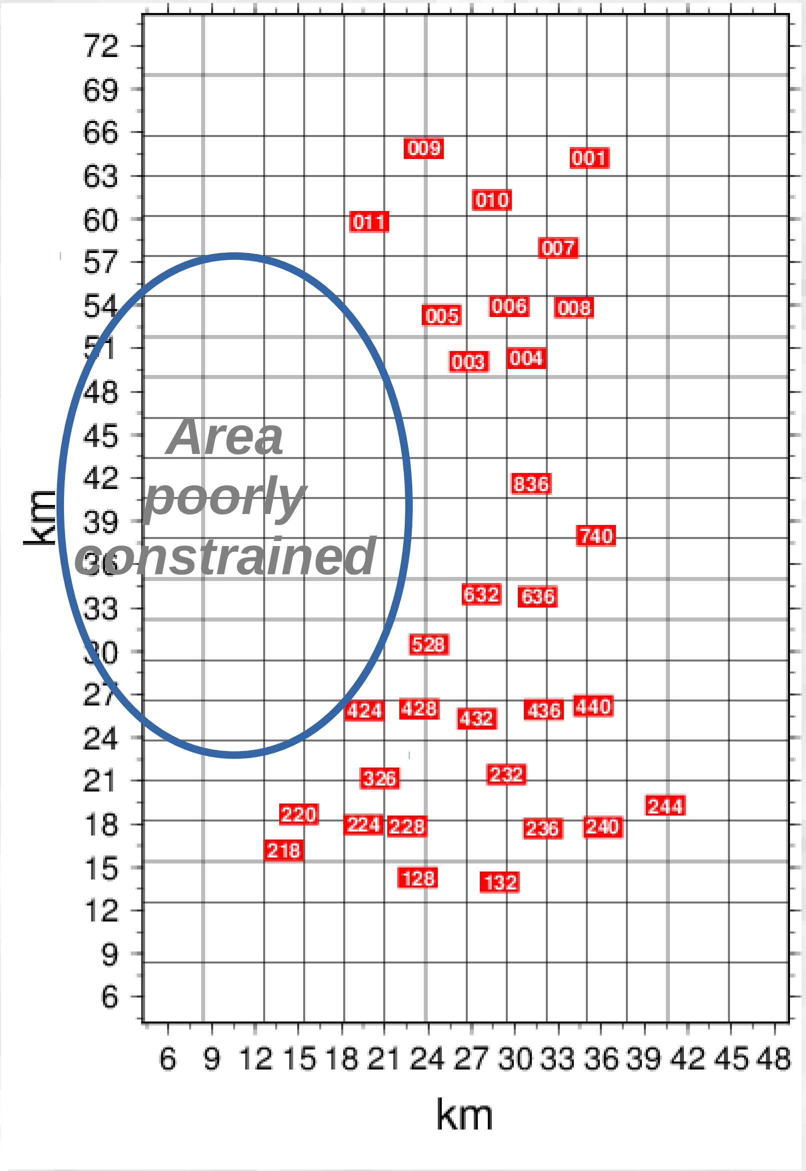

Non-regular array of MT sites: Case Study 1
The Omo Basin, South-West Ethiopia

Grid for Inversion

Uppermost layers

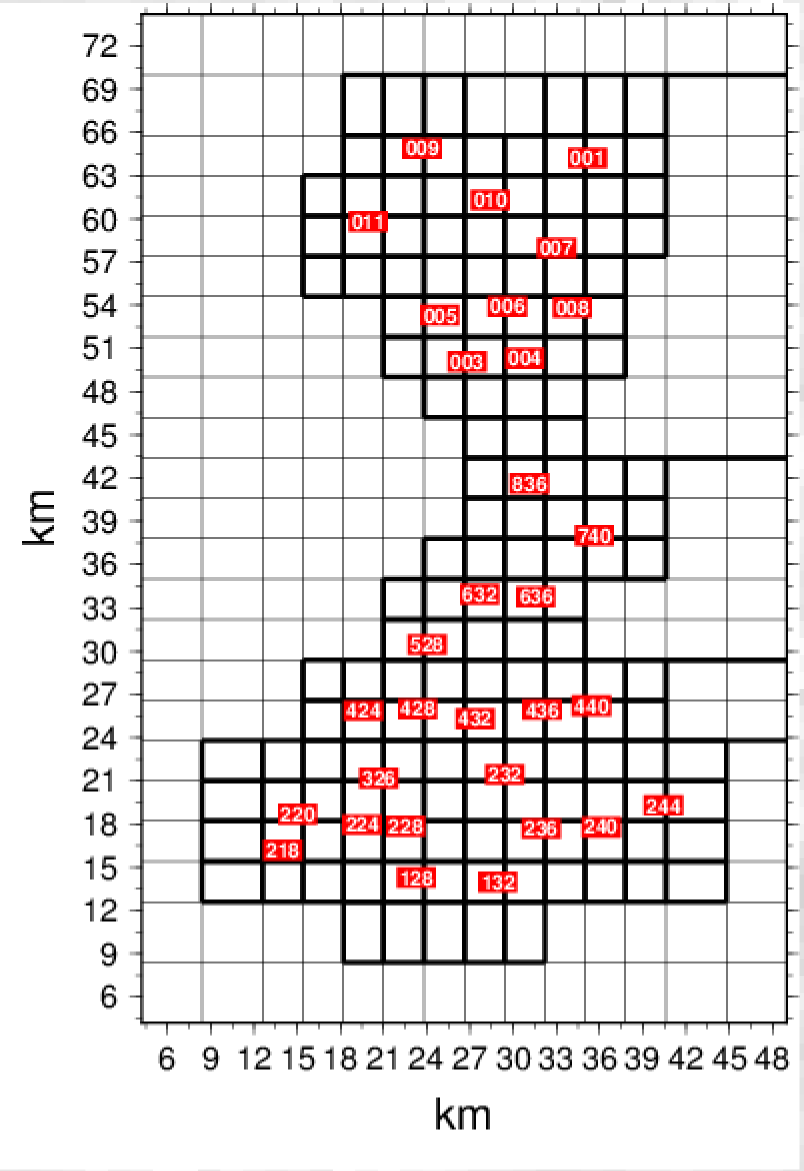

Non-regular array of MT sites: Case Study 1
The Omo Basin, South-West Ethiopia

Grid for Inversion

Intermediate layers

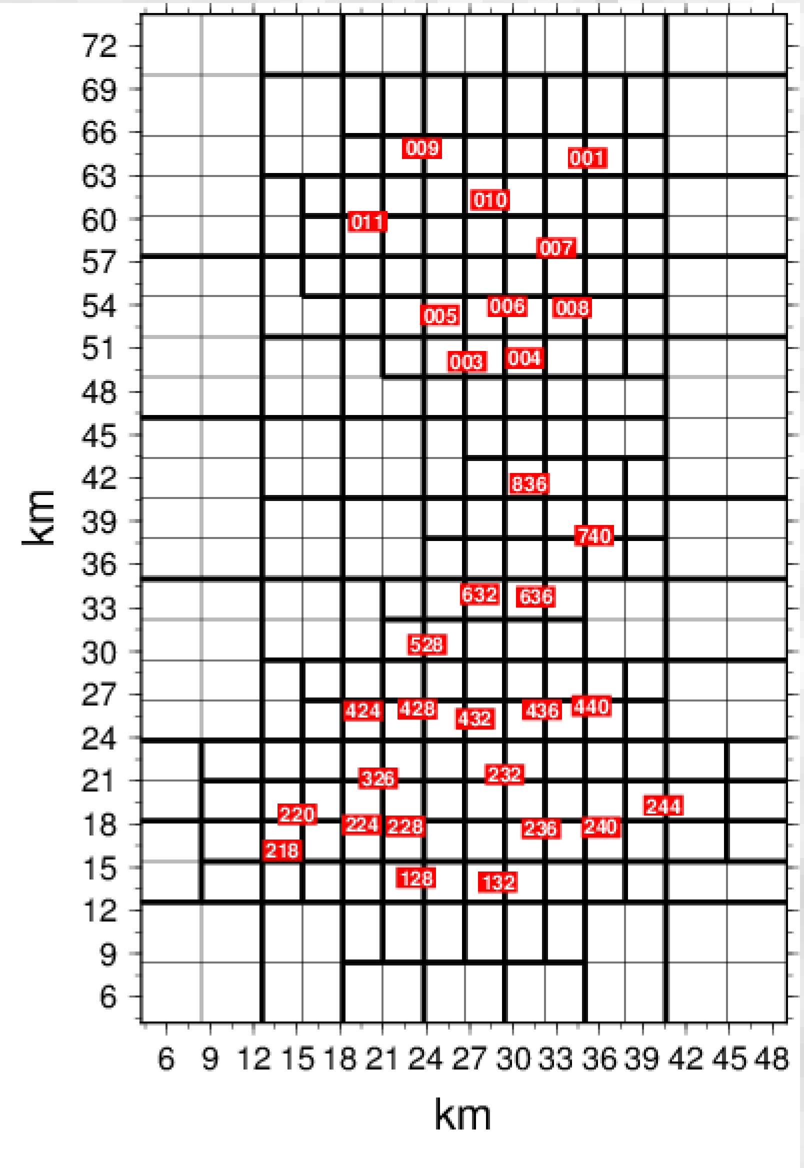

Non-regular array of MT sites: Case Study 1
The Omo Basin, South-West Ethiopia

Grid for Inversion

Deeper layers

(Depth >> size of the cells)

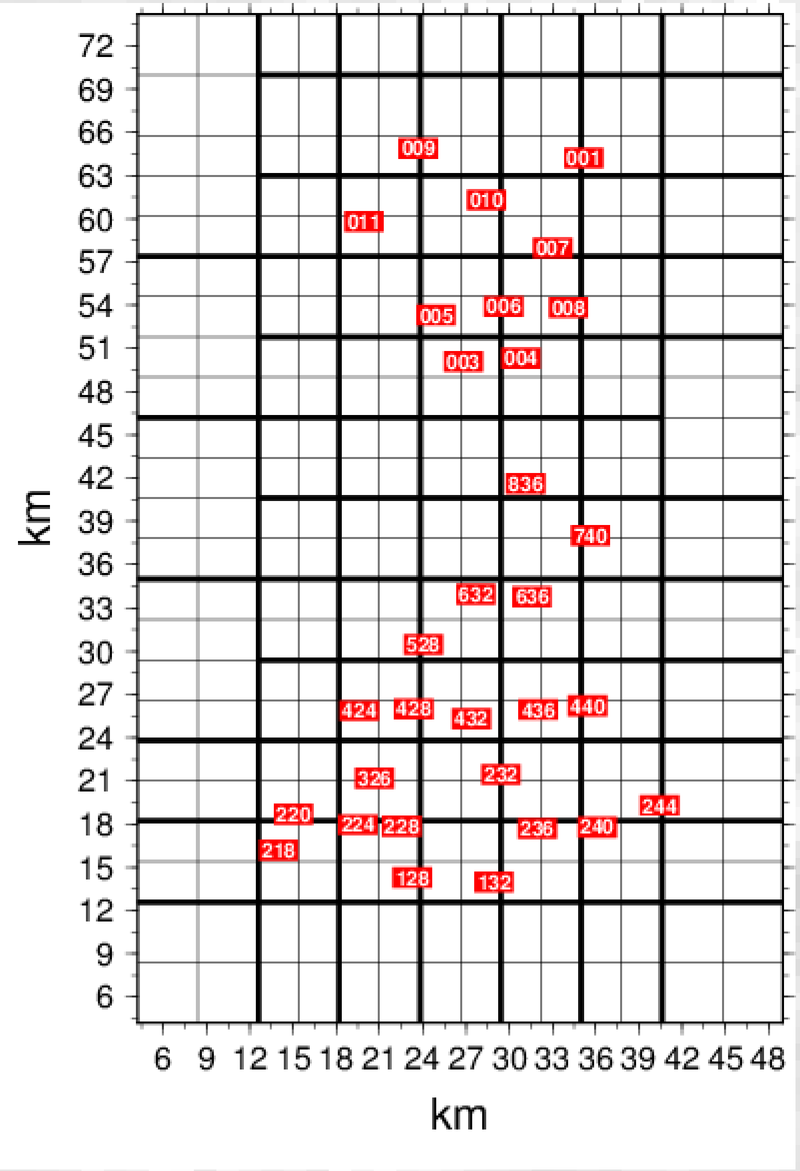

Non-regular array of MT sites: Case Study 1
The Omo Basin, South-West Ethiopia

Results

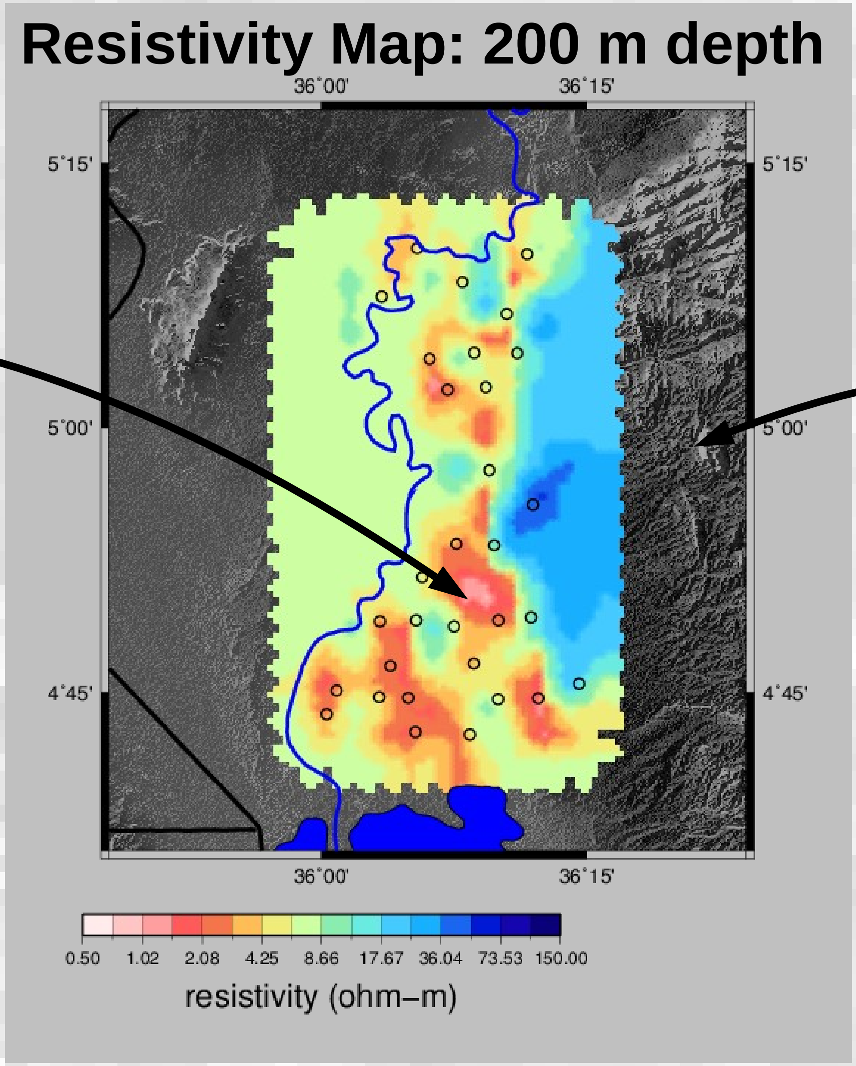

Sediment

Basement

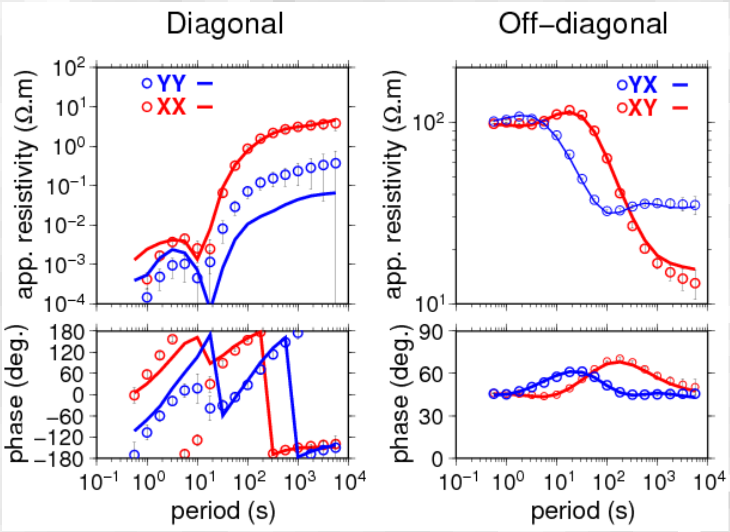

Non-regular array of MT sites: Case Study 1
The Omo Basin, South-West Ethiopia

Results

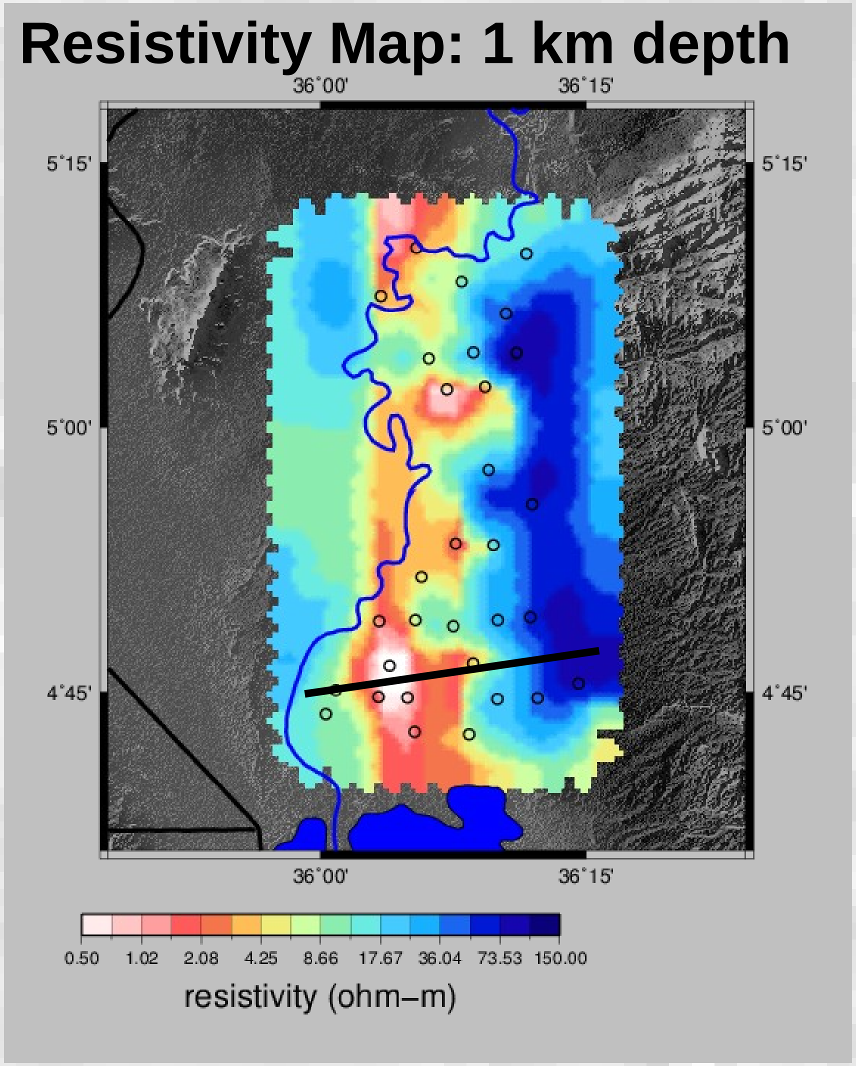

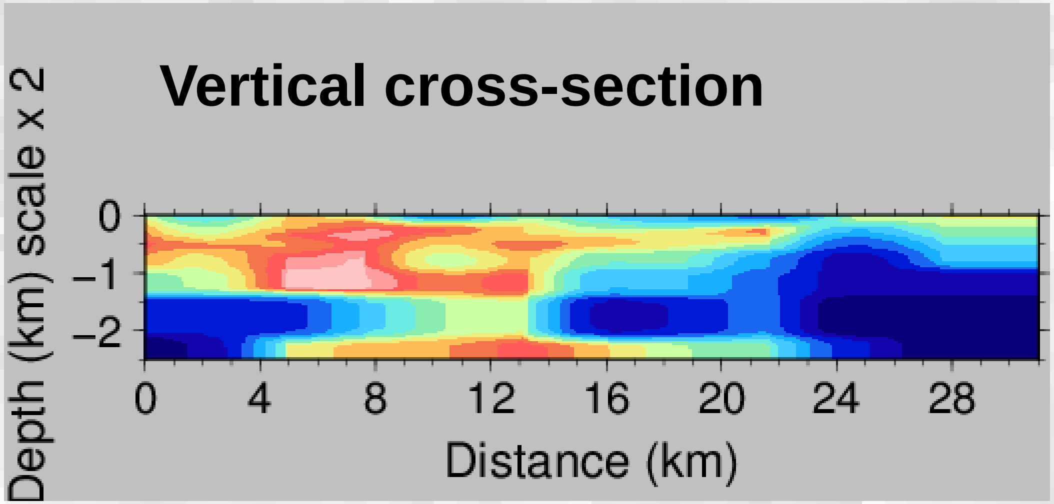

A step toward joint inversion

- **Objective function under consideration:**

$$D^2 = \sum_t \lambda_t \sum_n \frac{\left[M_n(t) - D_n(t)\right]^2}{\sigma_n^2(t)} + \sum_p \lambda_p S_p + \sum_c \lambda_c R, G$$

$$M_n(t) \Leftrightarrow R(p_{1,} \ldots, p_t), G(p_{1,} \ldots p_t)$$

  - **“t” techniques**
  - **“n” data per technique**
  - **“p” types of parameters**
  - **“M” model response and “D” data with error bars σ.**
  - **Weight the objective function according to data (“λ”)**
  - **S is a regularization term**

- **M may be interlinked between all parametres**
- **R for physical relationship**
- **G for geometrical constraint (ie cross-gradient)**

Testing constrained gravity inversion
As a joint inversion approach

Consider two parameters $a(x, y, z)$ and $b(x, y, z)$ with their gradients ∇a and ∇b. Define :

$$\mathbf{T} = \nabla a \times \nabla b \tag{1}$$

$$\|\mathbf{T}\| = \|\nabla a\| \|\nabla b\| |\sin\theta| \tag{2}$$

where θ is the angle between the vectors ∇a and ∇b.

$$\|\mathbf{T}\|^2 = |1 \pm \cos\theta|^2 \tag{3}$$

The minus term is for parallel while the plus term is for anti-parallel. The term $|\cos\theta|$ is obtained from the dot product $\nabla a \cdot \nabla$ b :

$$\cos\theta = \nabla a \cdot \nabla b / \|\nabla a\| \|\nabla b\| \tag{4}$$

Why jointly invert MT and gravity

- Relationship resistivity / density/ earth properties unknown (composition, fluids, temperature)
- Ambiguity to interpret conductor and resistor in depth
- Joint inversion with gravity identify light/dense material to conductor/resistor

Full Joint Inversion MT + Gravity (2-D)

- Synthetic MT data at 11 sites
- Gravity data at 80 points

Synthetic test in complex geological environment

Original Density model

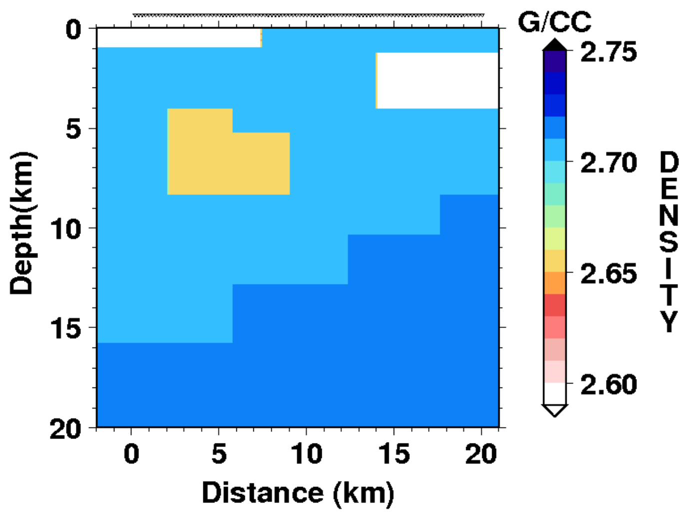

Original Resistivity model

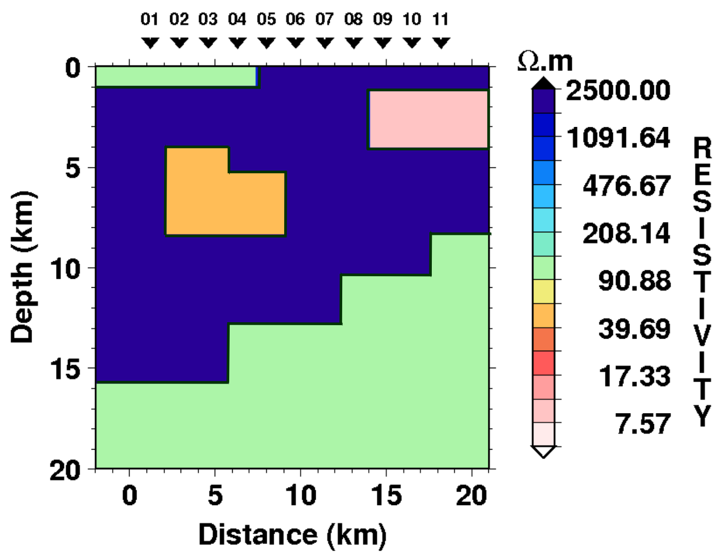

Abdelfettah al., 2010

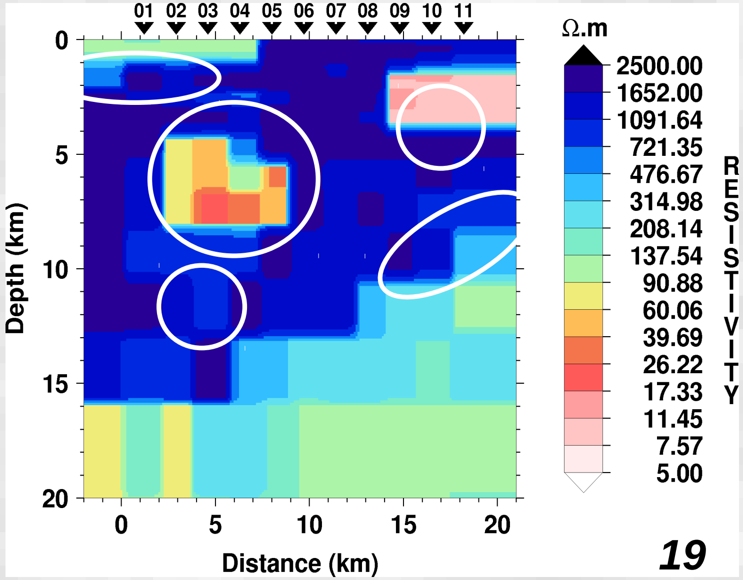

Resistivity

Joint Inversion

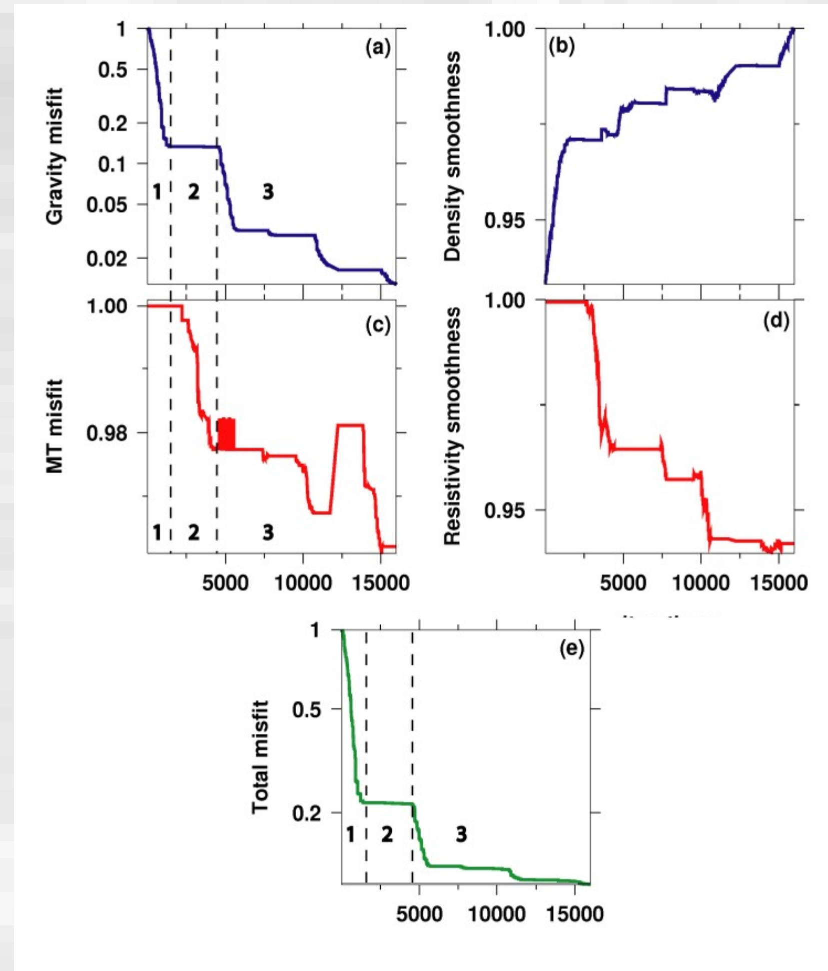

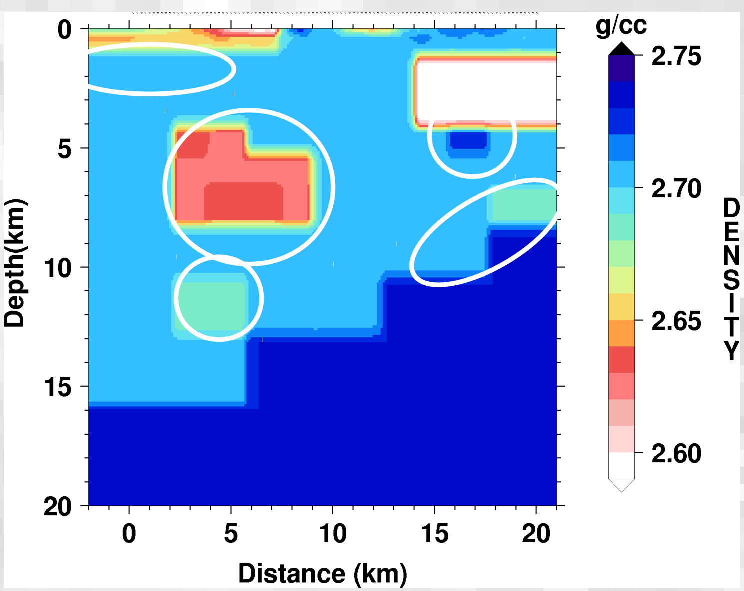

Density

Misfit evolution during inversion

Starting model – homogenous

MT and Gravity inversion of real data

Imaging the crust under Turkana rift, North Kenya
(Abdelfettah et al, en préparation)

Turkana basin for
- East African Rift evolution
- Associated sedimentary basins

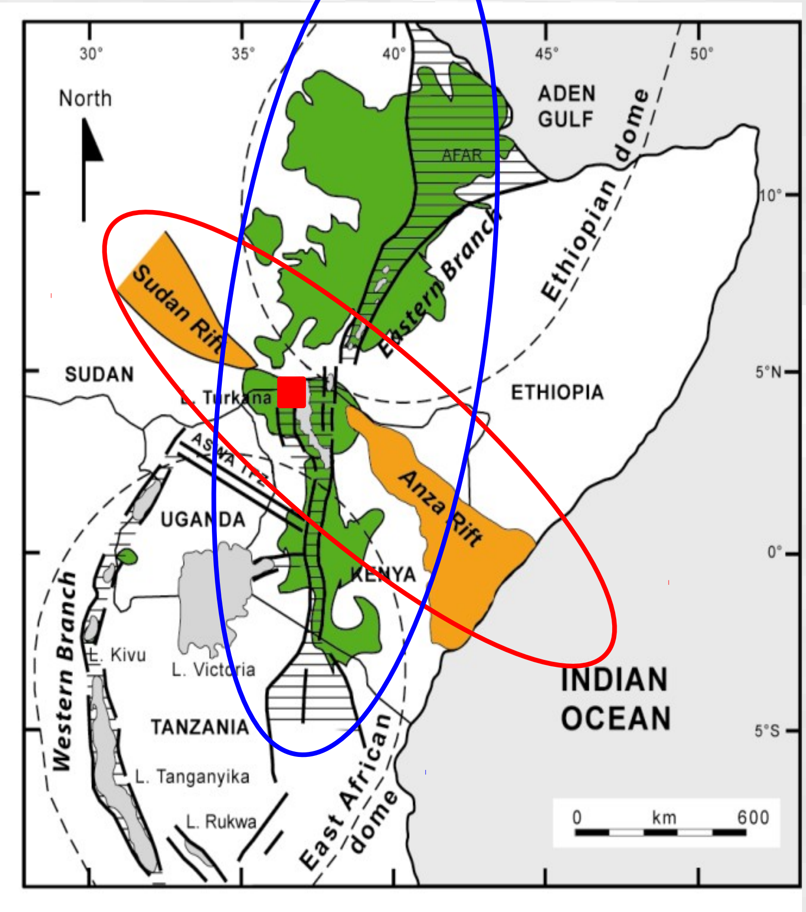

Le Gall et al., 2005

3-D MT model obtained for the whole area

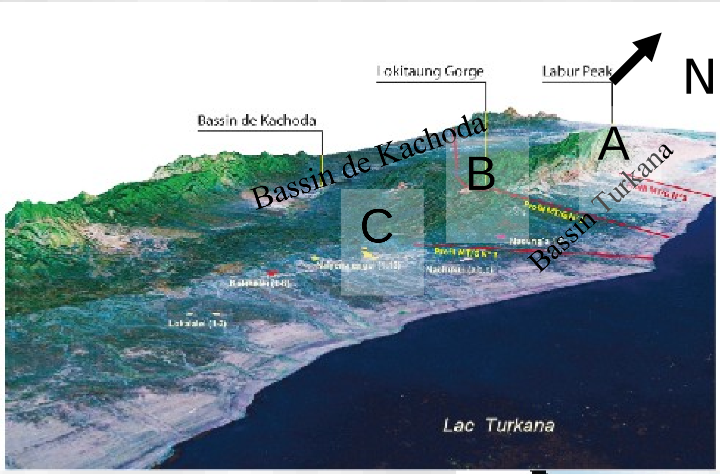

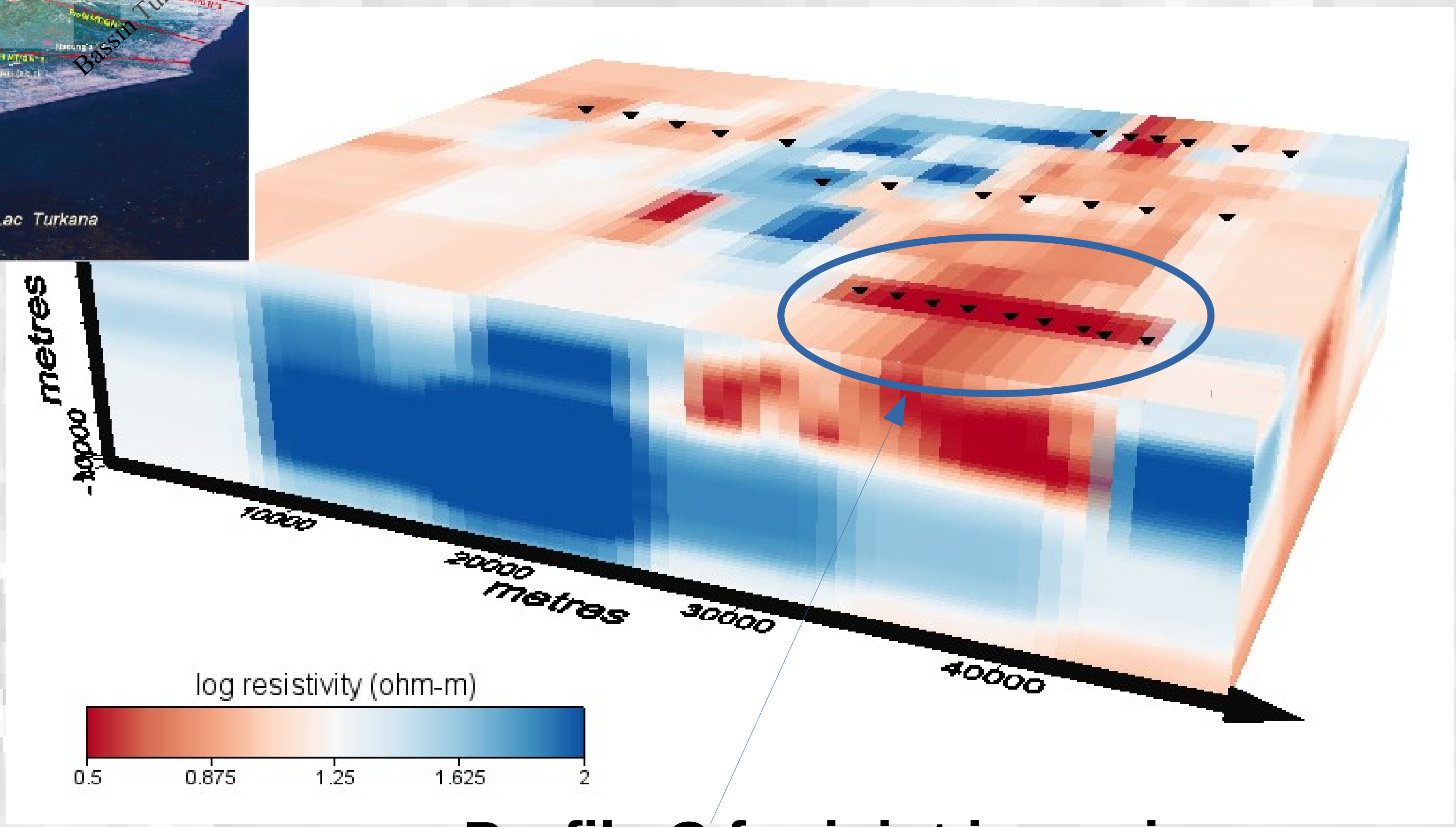

Profile C for joint inversion

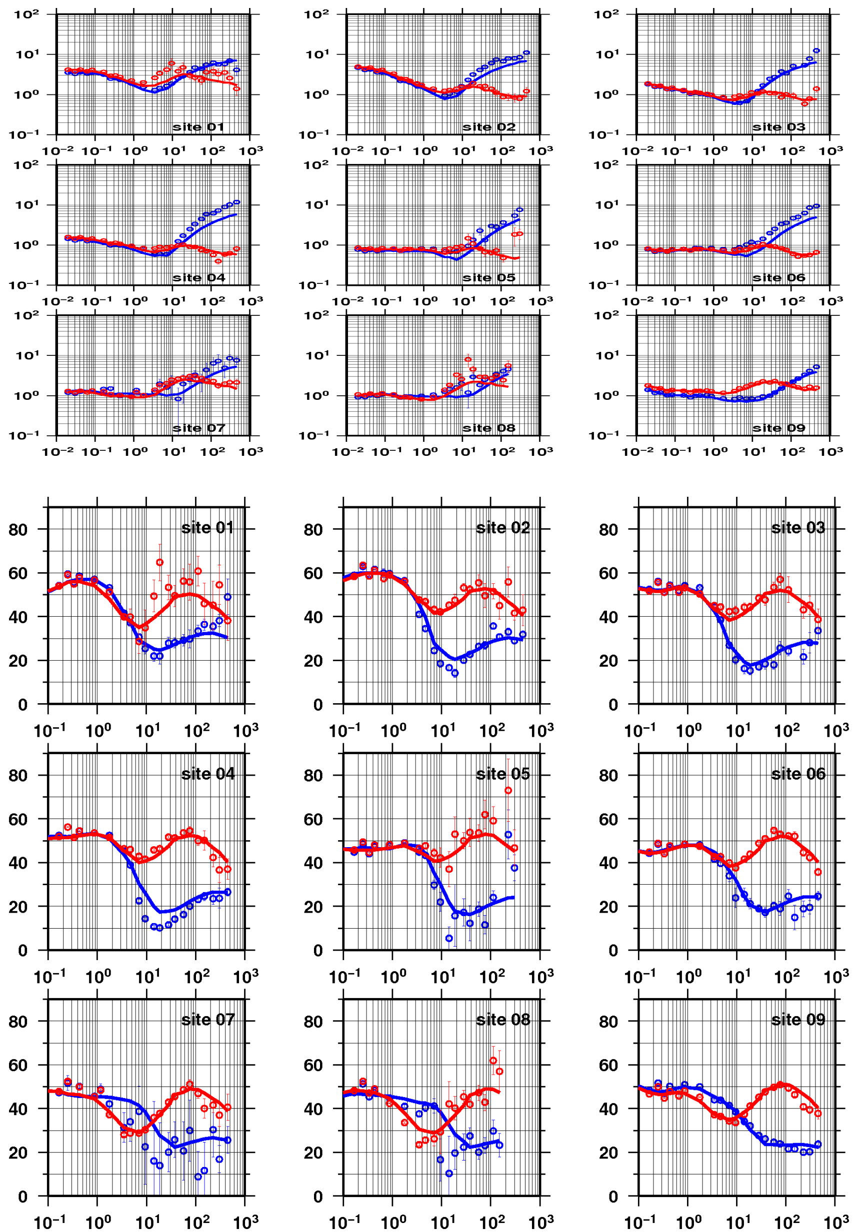

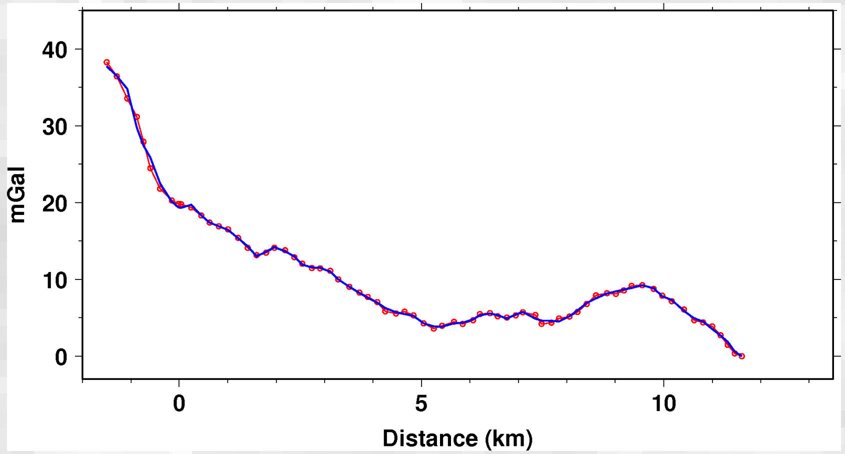

Joint inversion along profile : A selection of MT data (left) and gravity data (above)

The deep Resistivity and Density structure of the rift

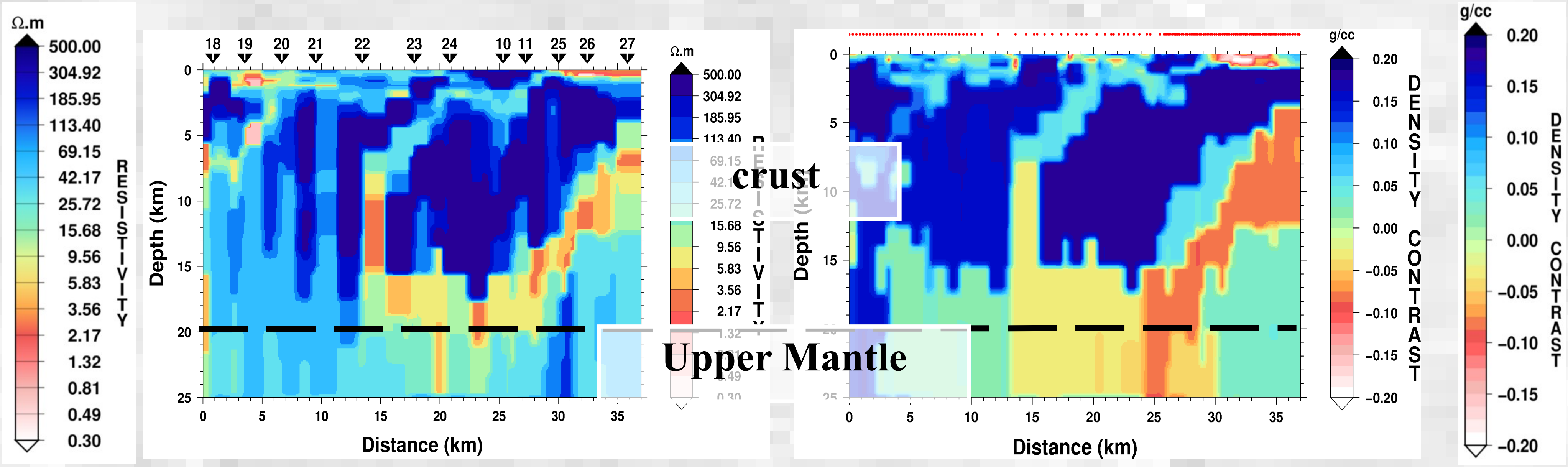

Resistivity and density values

→ > 20 km, ρ ϵ [20, 70] Ω.m

, δ ϵ [-0.05, 0.05] g/cm³

→ < 20 km, ρ ϵ [5, 500] Ω.m

, δ ϵ [-0.2, 0.2] g/cm³

Future joint inversion projects

The AFAR rift

- Joint inversion in gestation
  - Deformation measurement (GPS, interferometry)

- Difficulty
  - Multiple country project (UK, NZ, FR, US)
  - Availability of data
  - Expertise

Non-regular array of MT sites: Case Study
The Dabbahu Magmatic Rift Segment, Afar, Ethiopia

The Afar Triple Junction

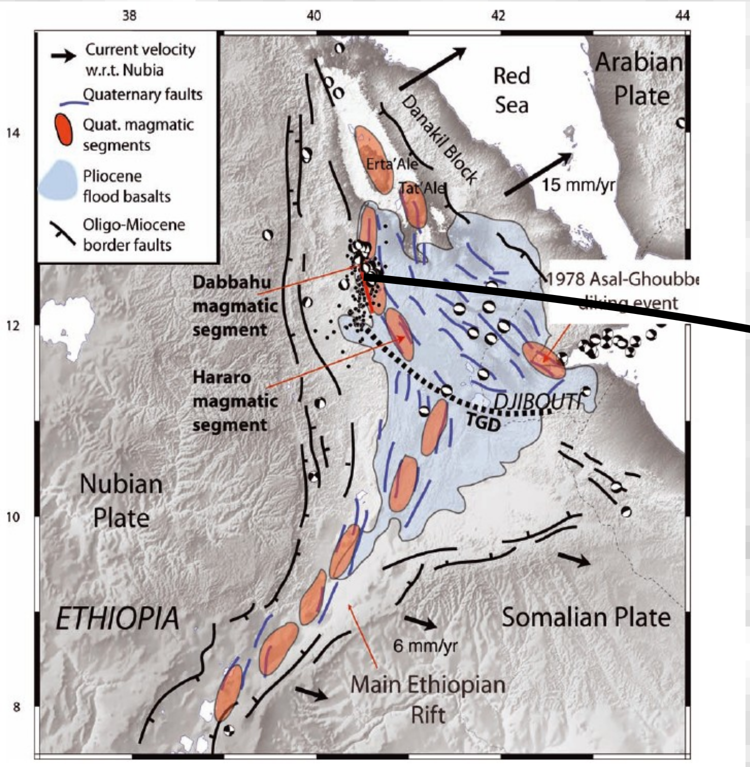

(Ebinger et al., 2008)

September 2005
The Dabbahu rifting episode

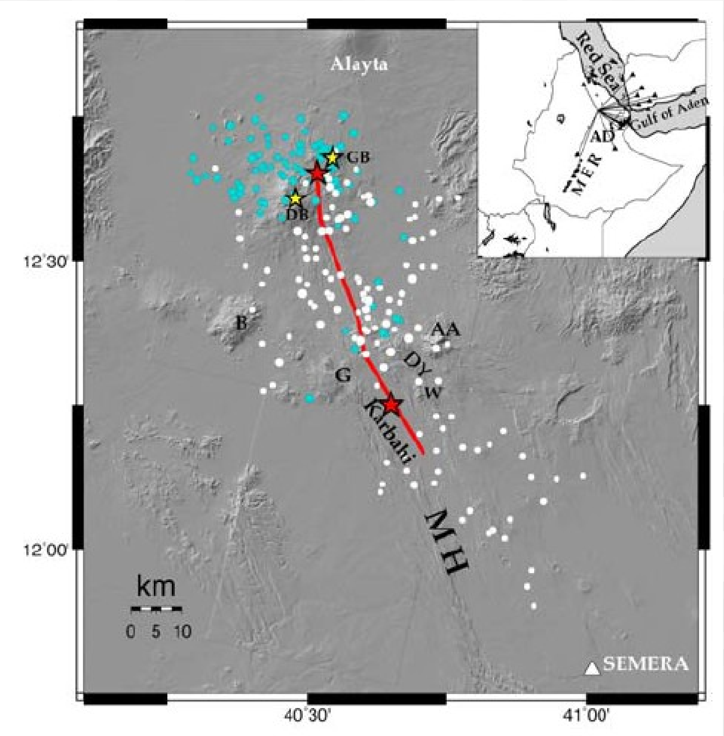

(Ayele et al., 2009)

- 2.5 km^3 of magma intruded along the entire length of the segment (60 km).
- 26/09: Eruption of the Dabbahu Volcano

Non-regular array of MT sites: Case Study 2
The Dabbahu Magmatic Rift Segment, Afar, Ethiopia

First Magnetotelluric survey in 2008 (< 3 years after the eruption)

Afar Rift Consortium (NERC funding)

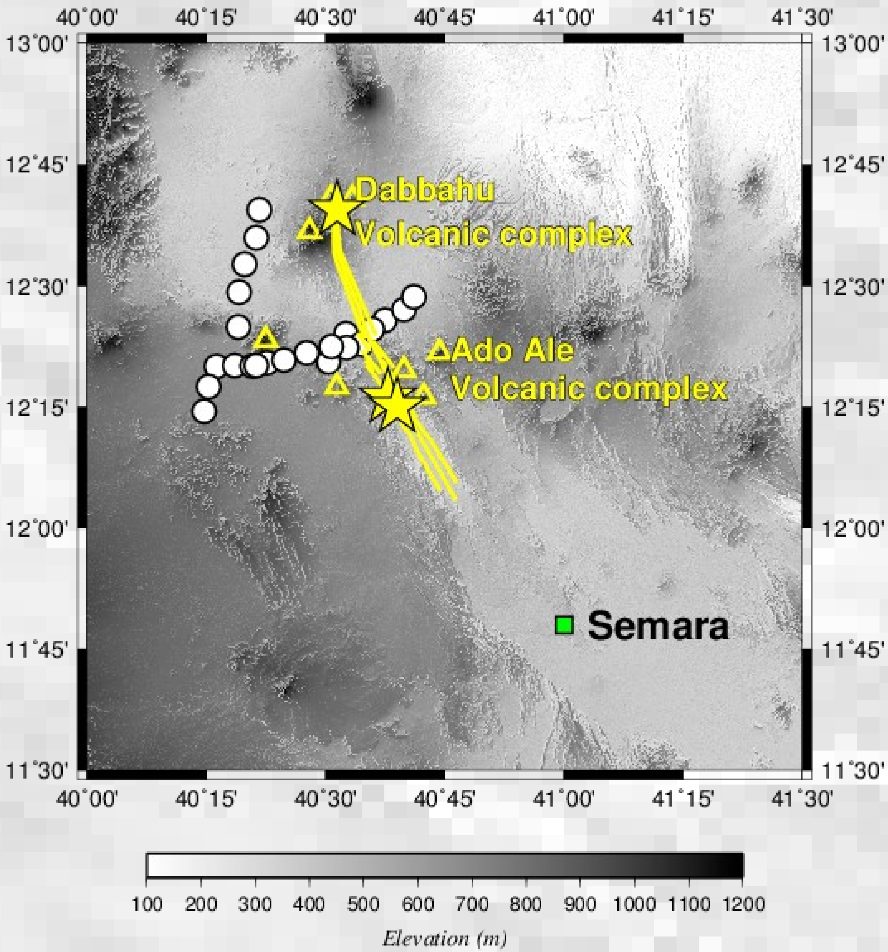

Non-regular array of MT sites: Case Study 2
The Dabbahu Magmatic Rift Segment, Afar, Ethiopia

Limited number of sites, due to field conditions

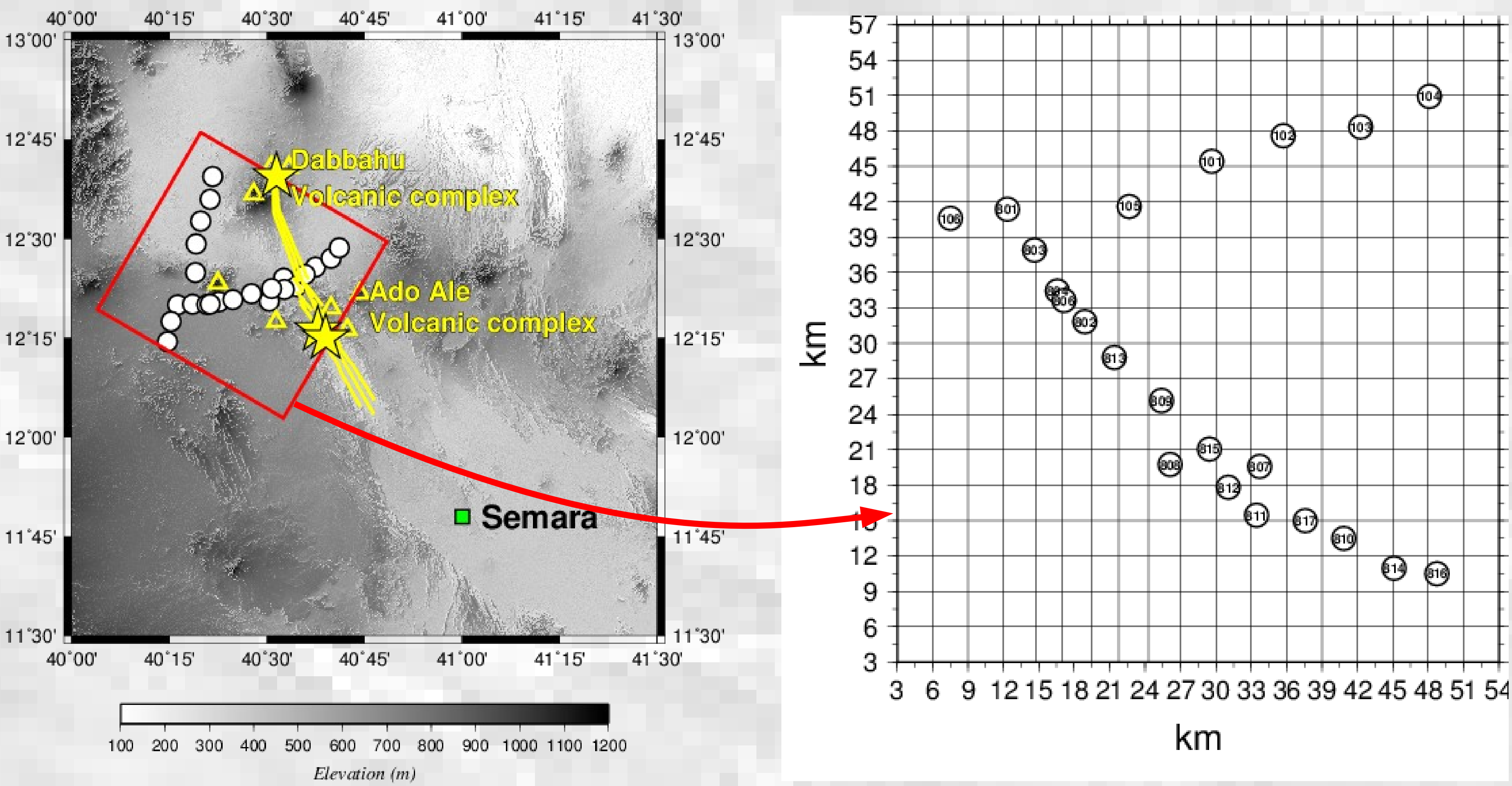

Non-regular array of MT sites: Case Study 2
The Dabbahu Magmatic Rift Segment, Afar, Ethiopia

Limited number of sites, due to field conditions: Adapted Grid for Inversion

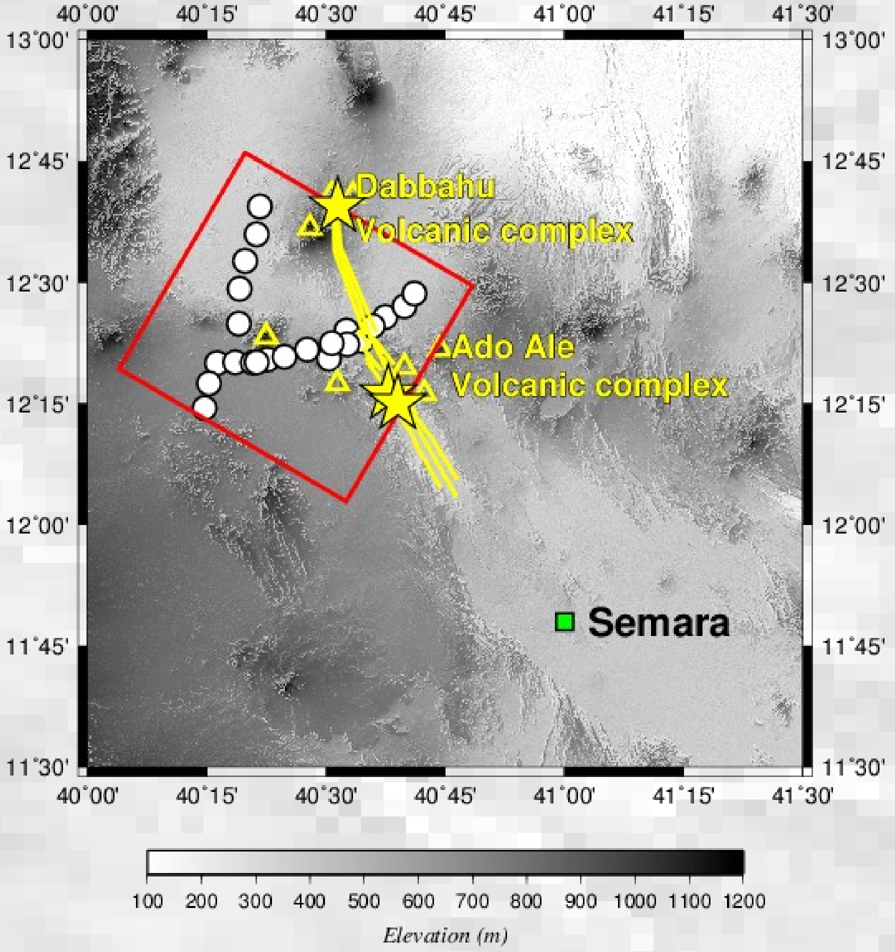

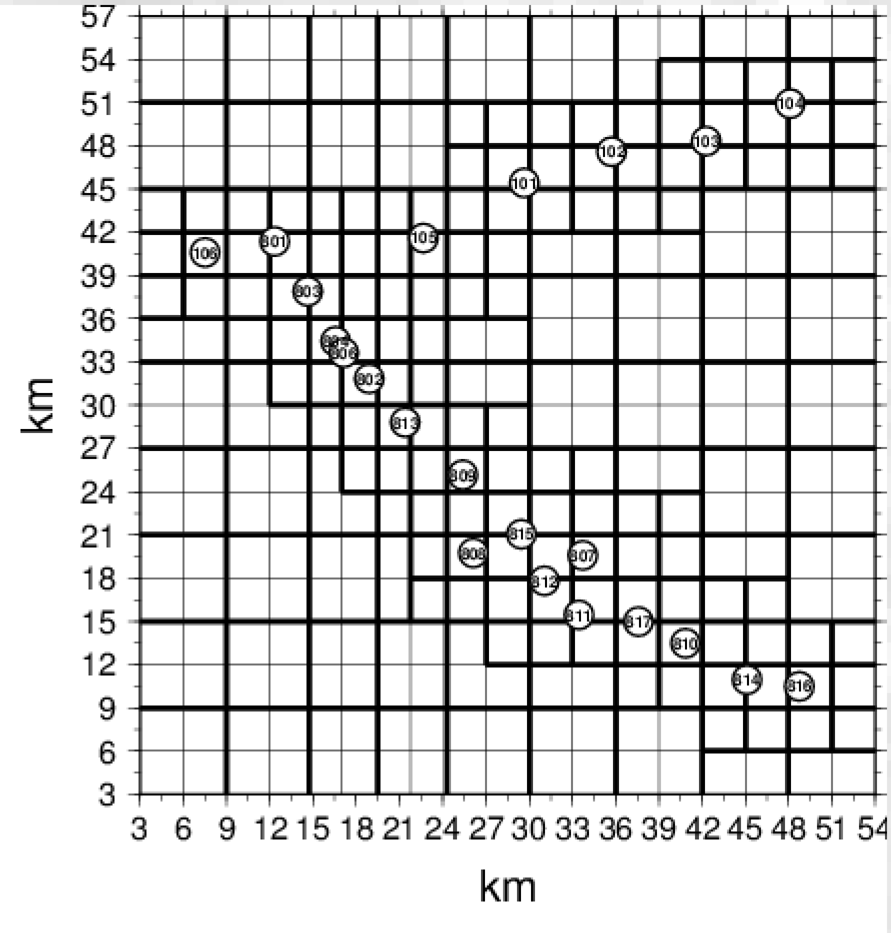

Non-regular array of MT sites: Case Study 2
The Dabbahu Magmatic Segment, Afar, Ethiopia

Results

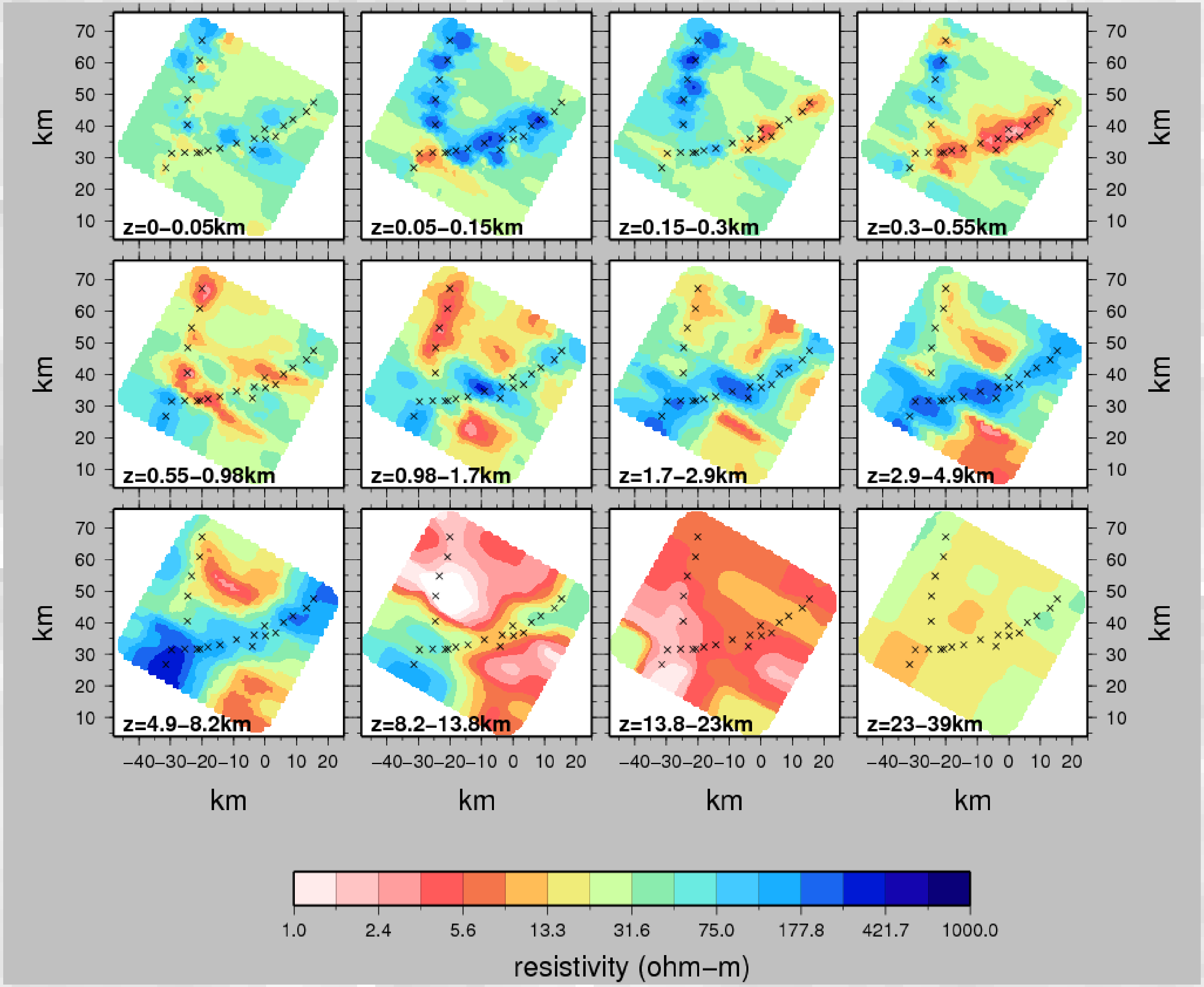

Non-regular array of MT sites: Case Study 2
The Dabbahu Magmatic Segment, Afar, Ethiopia

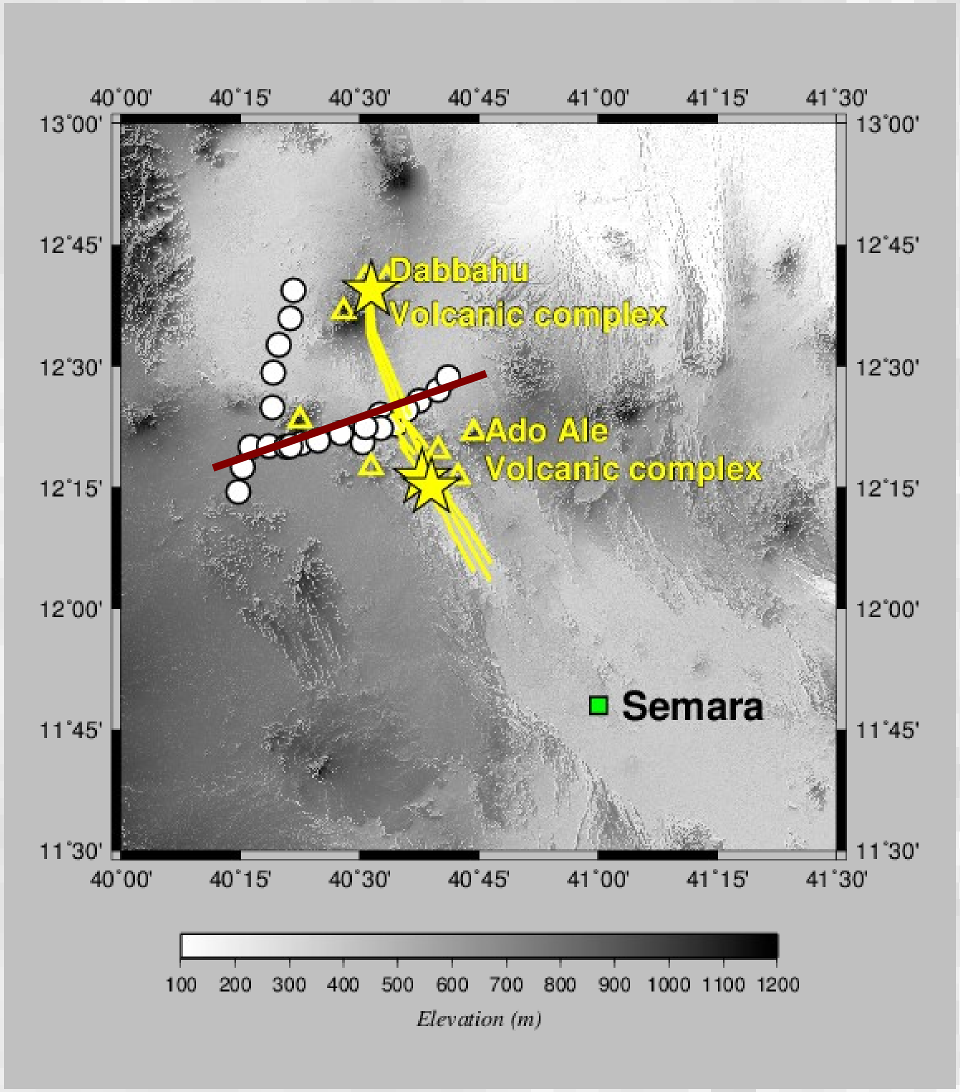

Results

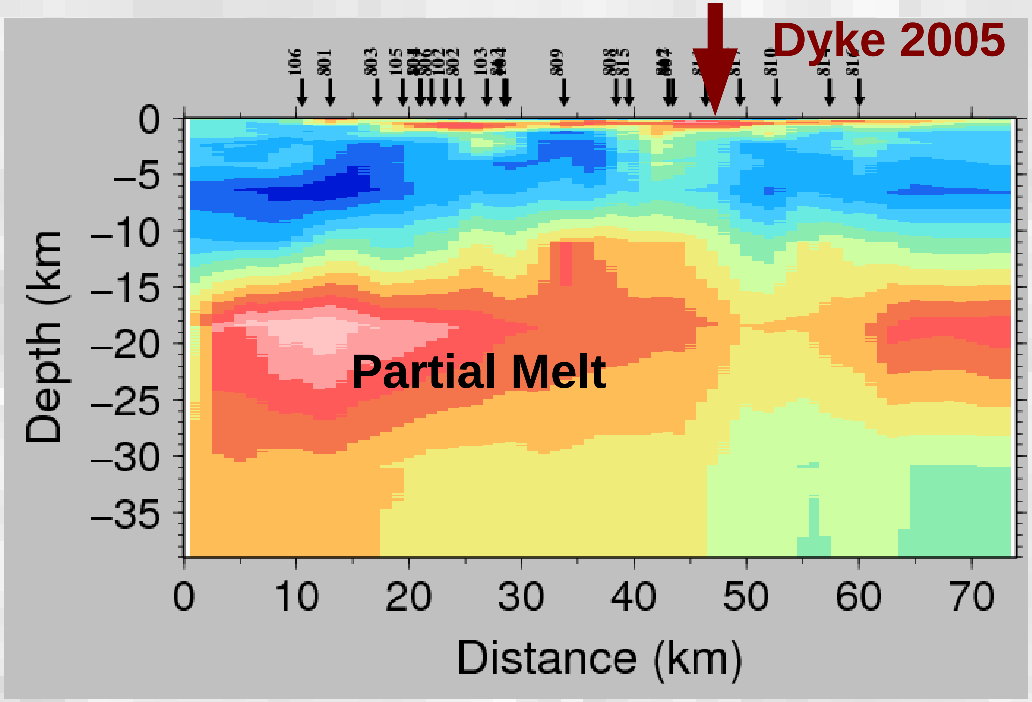

Non-regular array of MT sites: Case Study 2
The Dabbahu Magmatic Rift Segment, Afar, Ethiopia

Comparison with results from 2D Inversion

3D

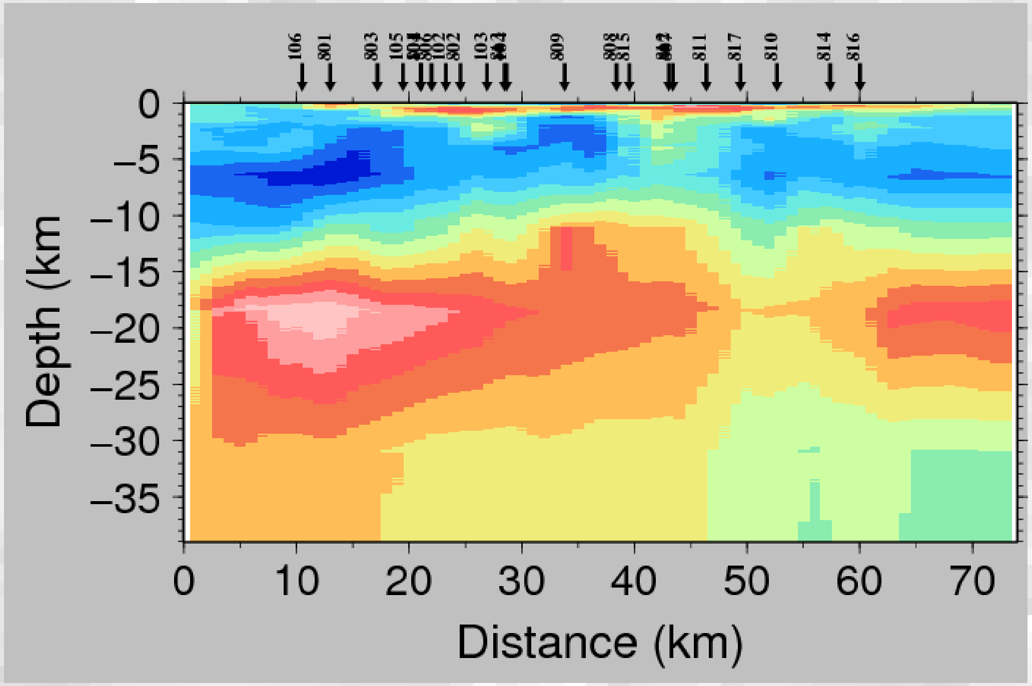

2D

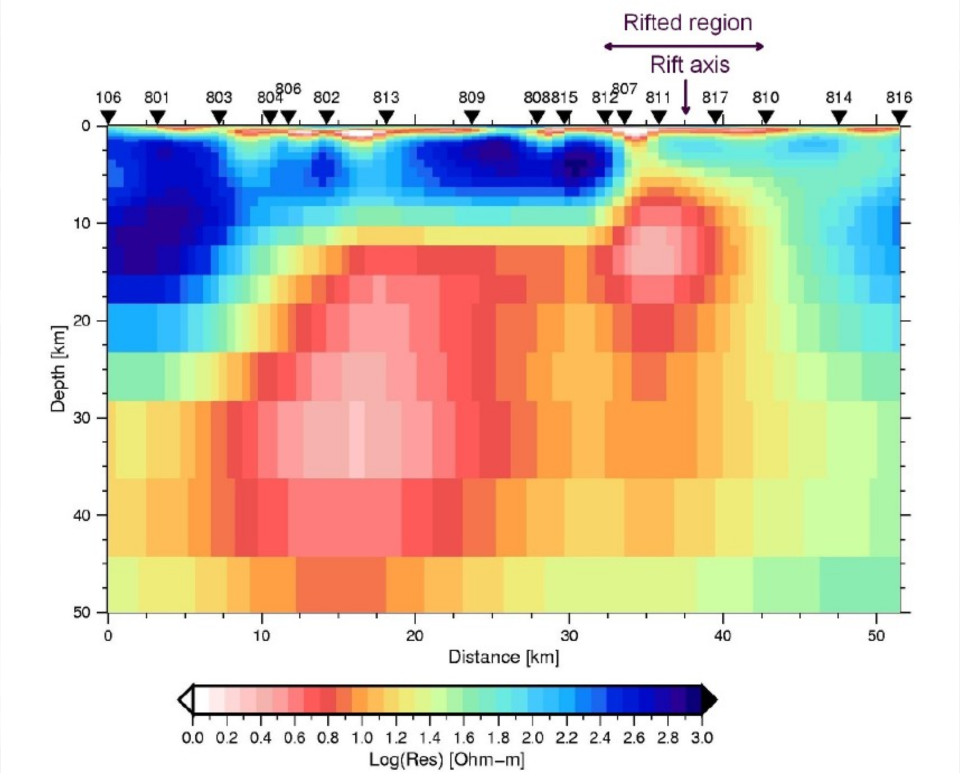

Only the 3-D inversion is suitable for joint inversion

(Desisssa et al., Nature Geoscience, 2013)

Three-dimensional electrical conductivity image of the mantle beneath the Society hotspot in the French Polynesia

Noriko Tada[1], Pascal Tarits[2], Takafumi Kasaya[1], Kiyoshi Baba[3], Daisuke Suetsugu[1] , Hisashi Utada[3]

[1]Japan Agency for Marine-Earth Science and Technology (JAMSTEC)

[2]Institut Universitaire Europeen de la Mer

[3]ERI, The University of Tokyo

- Joint inversion project
-
    - France/Japan cooperation
    - Seismology must be published
    - Competition
    - Availability of data

Seismic Tomography

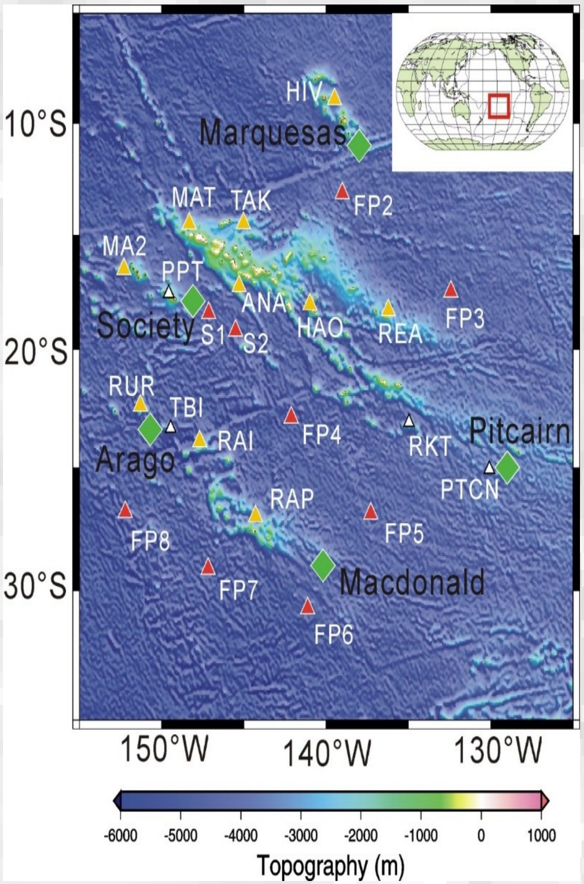

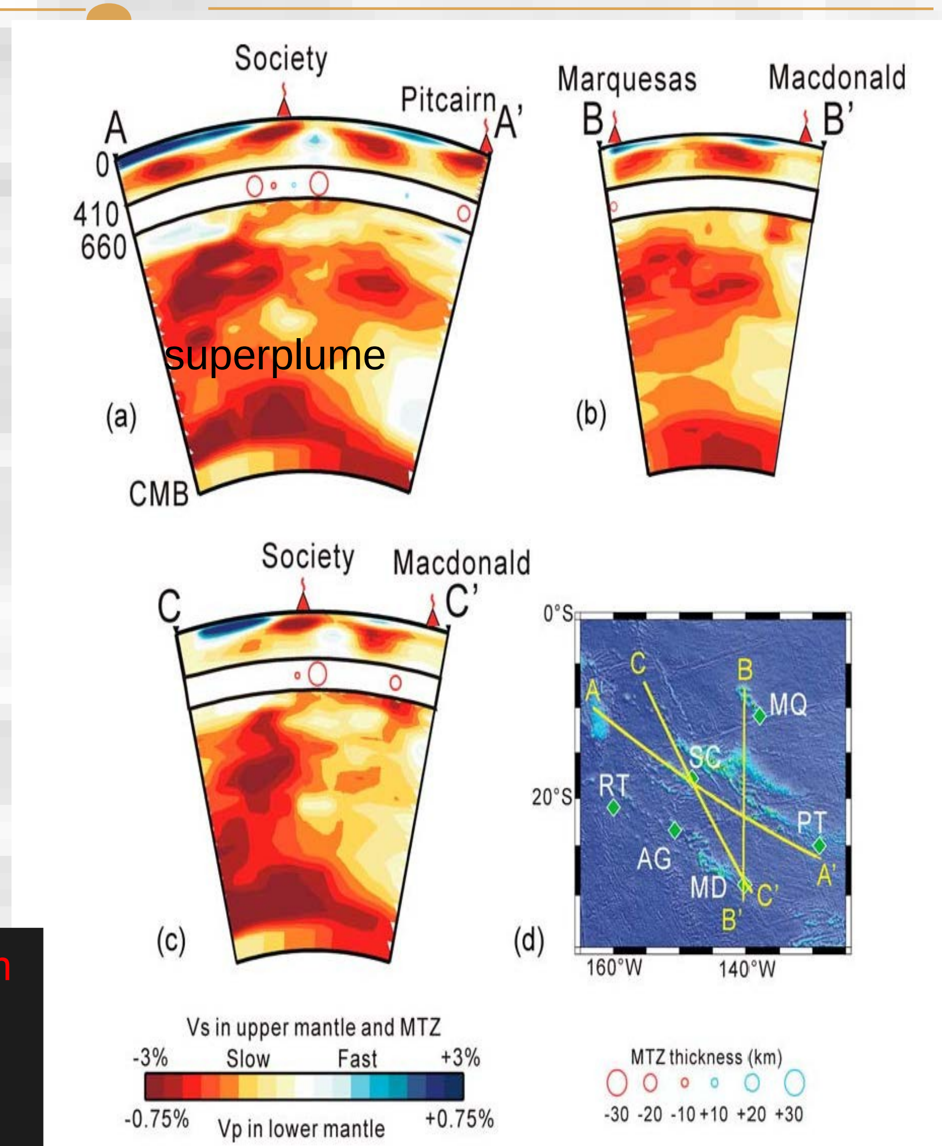

Red: BBOBS (Broadband Ocean-Bottom Seismometer) stations (seafloor)
Yellow: French PLUME stations (island)
White: Permanent stations (island)
Green: Hotspots

Suetsugu et al. (2009)

Previous MT Study (Nolasco et al., 1998)

Direction of
plate spreading

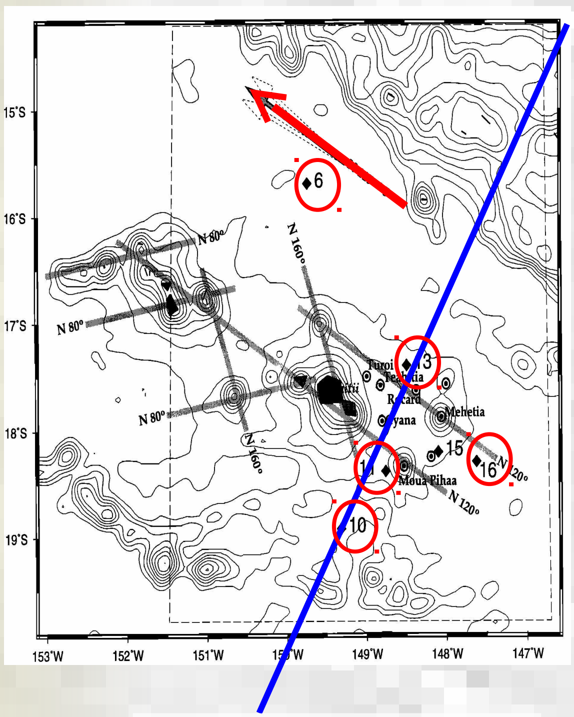

2-D cross section

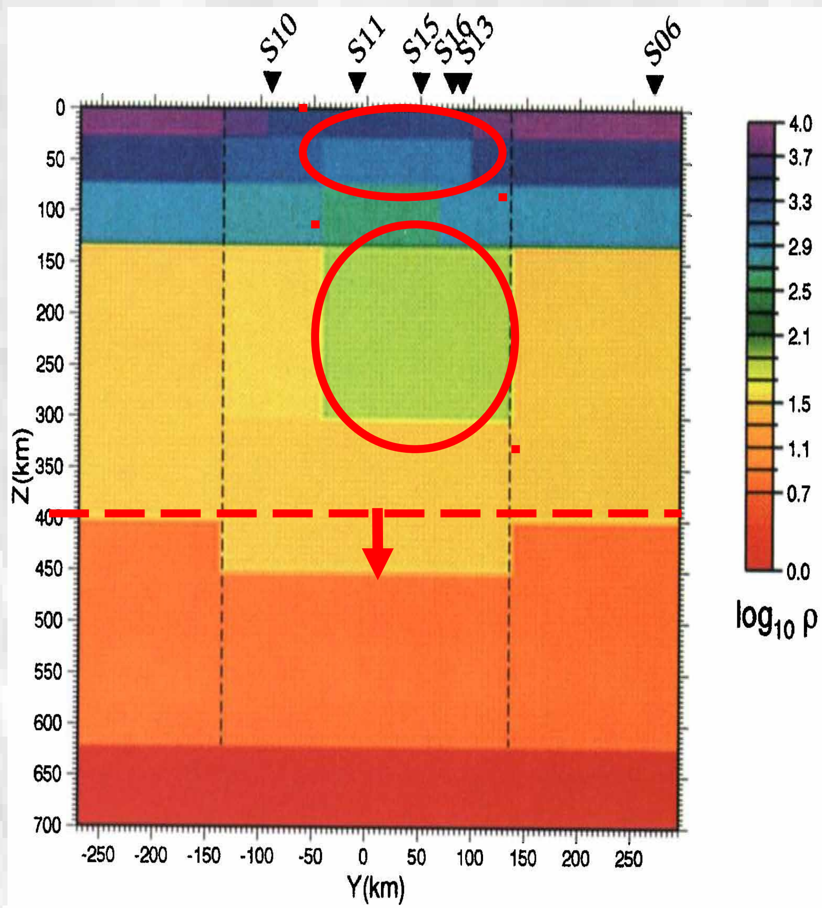

- 2-D electrical conductivity model was estimated using 5sites.
- The conductive anomaly is located at ~50 km depth.
- The resistive anomaly is located at 150-300 km depths.
- Discontinuity at 410 km shifts to deeper part.

TIARES Project

(Tomographic Investigation by seafloor ARray Experiment for Society hotspot)

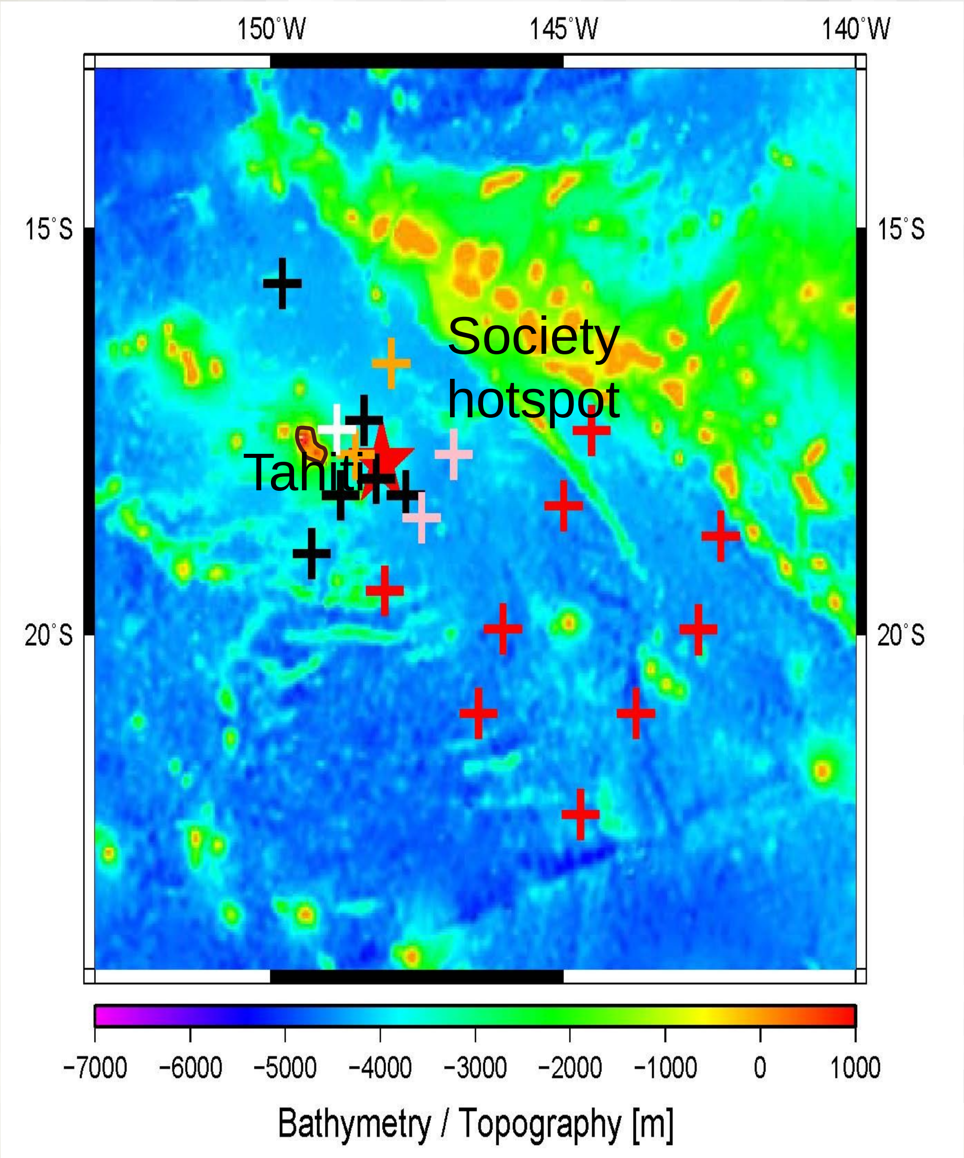

- Reveal detailed 3-D image of mantle plume beneath the Society hotspot by using OBEMs
- Observation Period: 2009-2010
- Japan-France cooperative project
  - \+ :9 Japanese OBEM sites
  - \+ :2 French OBEM sites
  - \+ +(E only) +(M only) :9 old sites

(Nolasco et al., 1998)

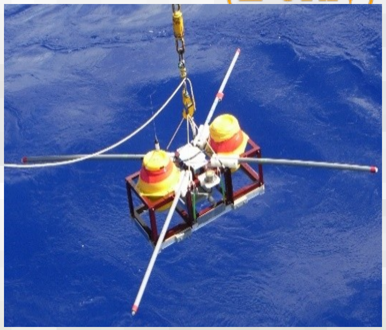

Japanese Ocean Bottom Electromagnetmeter (OBEM)

3-D Inversion Analysis

- Calculate MT responses from the observed data
  - BIRRP ver.5.1 (Chave and Thomson, 2003)

- Estimate averaged 1-D model as a background model of 3-D MT inversion
  - 1-D Occam's inversion (Constable et al., 1987)
  - Iterative method of correcting topographic effect (Baba et al., 2010)

- 3-D MT inversion
  - WSINV3DMT for marine MT (Tada et al., 2012; Baba et al., 2013)
  - 640 – 163,840 seconds (17 periods)
  - Calculation area: 5,000 km × 5,000 km× 1,020.80 km
  - The horizontal mesh size in the center of calculation area: 26 km
  - The horizontal mesh size for small-scale topographic correction: 1km in the central 7 km × 7 km
  - The vertical mesh size: 1 km near seafloor and wider as getting deeper
  - 71 × 71 × 50 (+7 air layers) blocks
  - The conductivity of seawater : 3.2 S/m
  - Topography data
    - 1-minute grid from ETOPO1 (NOAA)
    - 200-m grid from Multi-narrow beam sounding data collected by research cruises of JAMSTEC

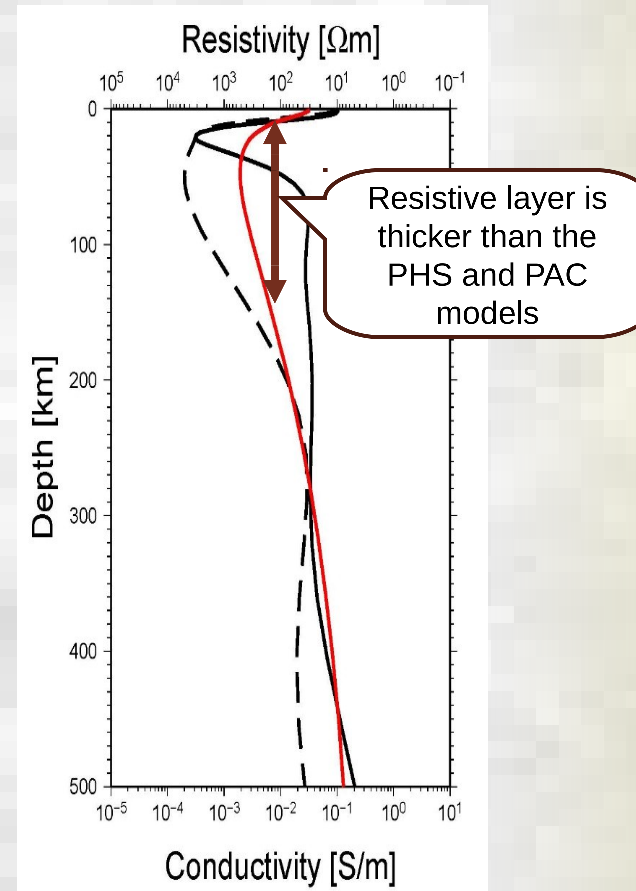

Averaged 1-D model
Red: South Pacific (70 Ma; This study)
Solid line: PHS (10-70 Ma; Baba et al., 2010)
Broken line: PAC (150 Ma; Baba et al., 2010)

Mesh Design

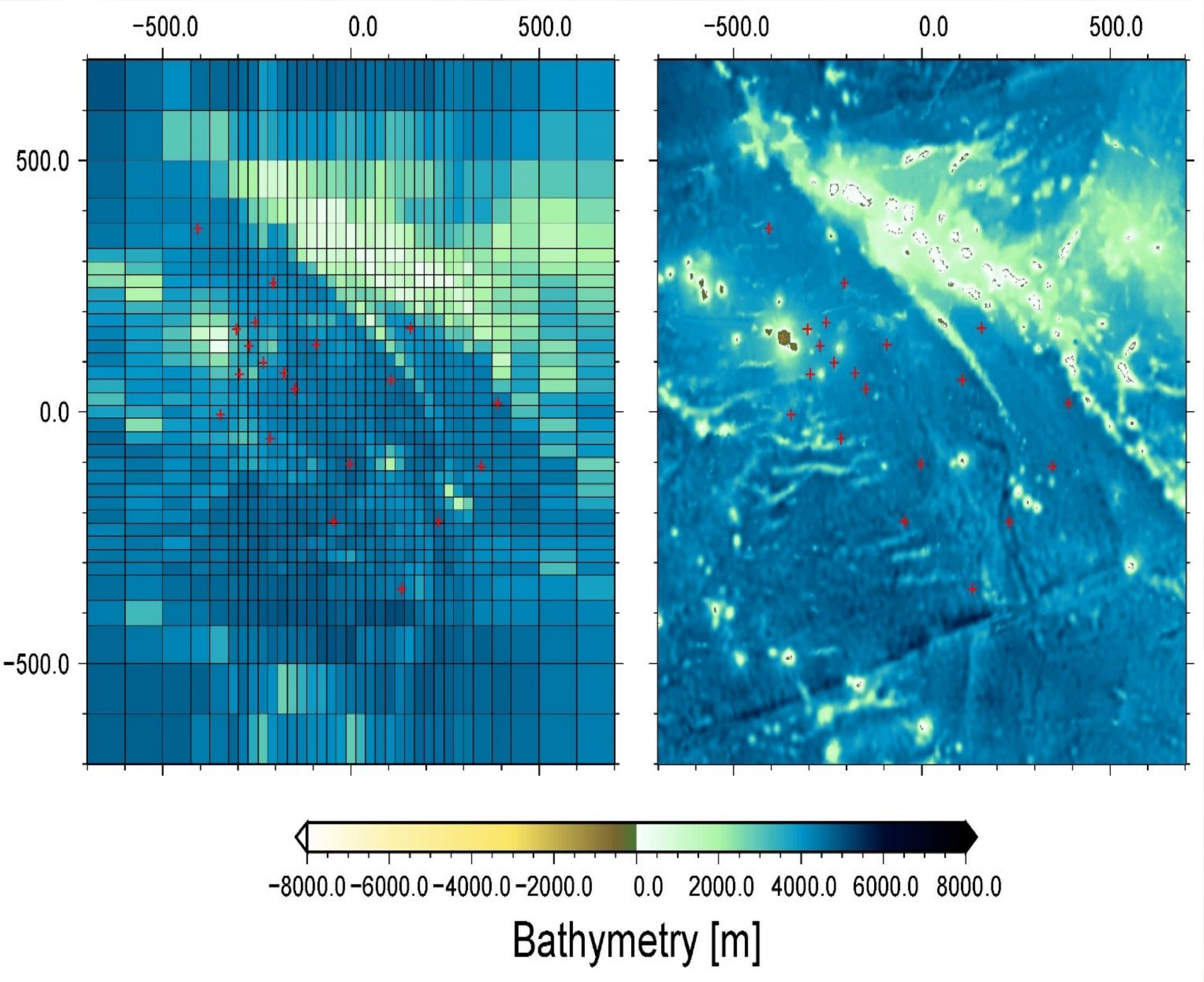

−500.0
0.0
500.0
−500.0
0.0
500.0
500.0
0.0
−500.0
−8000.0 −6000.0 −4000.0 −2000.0 0.0 2000.0 4000.0 6000.0 8000.0
Bathymetry [m]

Incorporation of Topography

- We separate treatment of the effects of regional large-scale and local small-scale topographies.
  - Regional large-scale topography (Tada et al., 2012)
    - Incorporate topographic variation into the initial model of the inversion program by conserving conductance in each block.
  - Local small-scale topography (Baba et al., 2013)
    - Incorporated by a distortion matrix of MT impedance tensor.

$$\sigma_h = \frac{\sigma_s V_s + \sigma_c V_c}{V_s + V_c}$$

$$Z^{ts}(\boldsymbol{r},T) = \boldsymbol{D}^{lt}(\boldsymbol{r},T)\boldsymbol{Z}^{rs}(\boldsymbol{r},T)$$

$\boldsymbol{Z}^{ts}$: MT response to full scale structure including local and regional topography.
$\boldsymbol{D}^{lt}$: Distortion due to local small-scale topography. 2 ×2 complex tensor.
$\boldsymbol{Z}^{rs}$: MT response including regional large-scale topography.

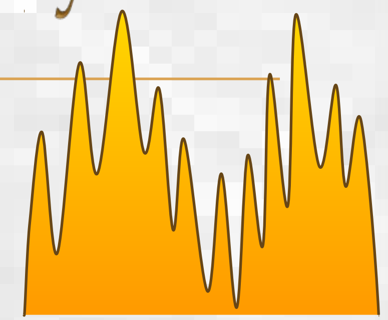

Real topography

=

Large-scale topography

+

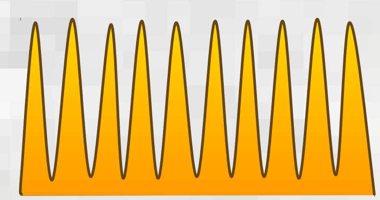

Small-scale topography

3-D Electrical Resistivity Model

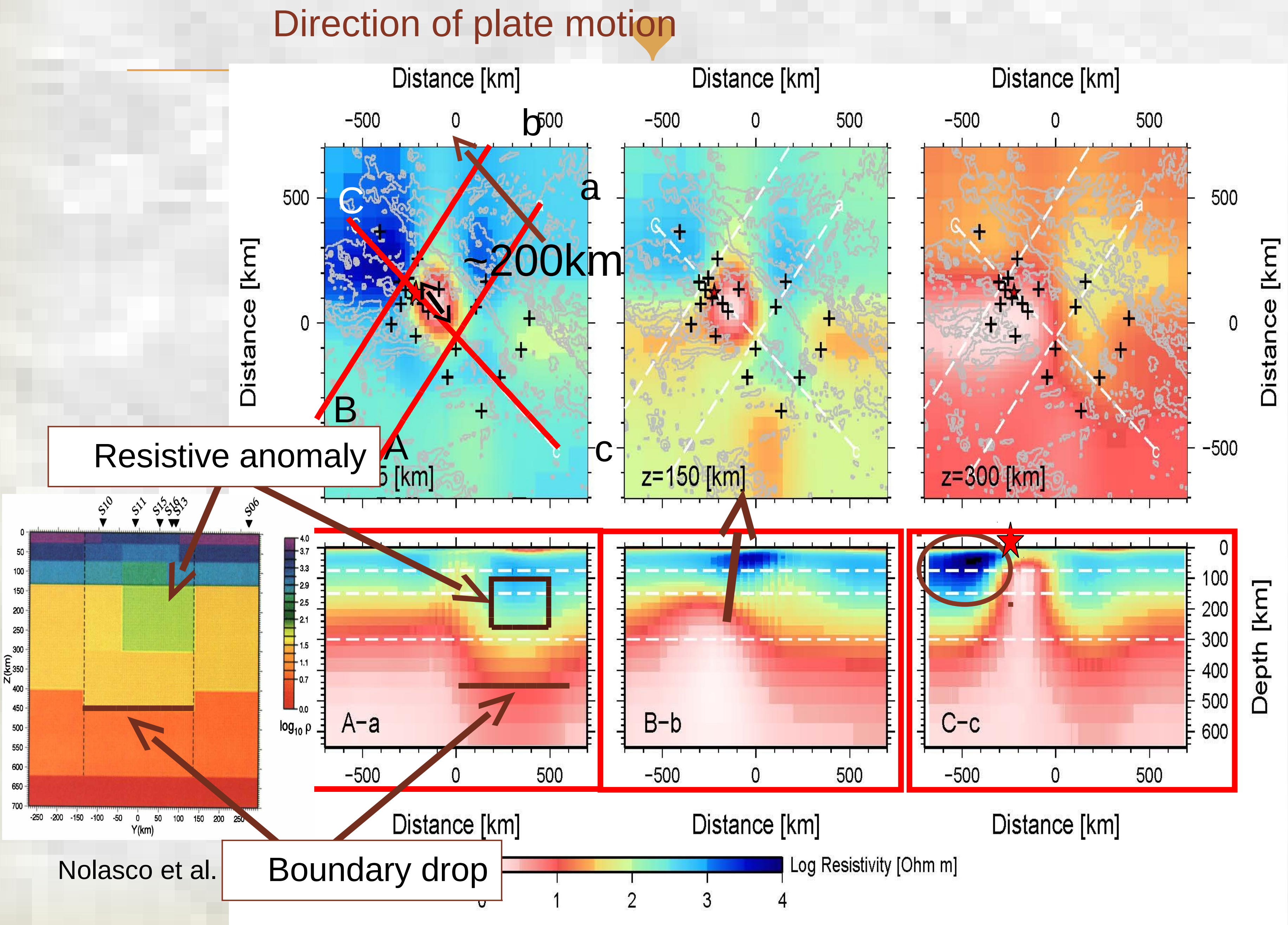

Nolasco et al.

In summary

- Relationship resistivity / earth properties unknown (composition, fluids, temperature)
- Ambiguity to interpret conductor and resistor in depth
- Same question in seismology (slow vs fast)
- Joint inversion with gravity identify light/dense material to conductor/resistor
- Joint inversion with seismology addresses composition/temperature ambiguity
- Large multiple country project complicates the joint inversion